Evidence That β-Tubulin Induces a Conformation Change in the Cytosolic Chaperonin Which Stabilizes Binding: Implications for the Mechanism of Action[†,‡]

Jane K. Dobrzynski,[§] Mona L. Sternlicht,[§] Isaac Peng,[||] George W. Farr,[⊥] and Himan Sternlicht*[,§]

Department of Pharmacology, Case Western Reserve University, Cleveland, Ohio 44106, Department of Neuroscience and Cell Biology, Robert Wood Johnson Medical School, University of Medicine and Dentistry of New Jersey, Piscataway, New Jersey 08854, and Department of Genetics and Howard Hughes Medical Institute, Yale University School of Medicine, New Haven, Connecticut 06510

Received September 9, 1999; Revised Manuscript Received February 7, 2000

ABSTRACT: The class II chaperonin CCT facilitates protein folding by a process that is not well-understood. One striking feature of this chaperonin is its apparent selectivity in vivo, folding only actin, tubulin, and several other proteins. In contrast, the class I chaperonin GroEL is thought to facilitate the folding of many proteins within *Escherichia coli*. It has been proposed that this apparent selectivity is associated with certain regions of a substrate protein's primary structure. Using limiting amounts of β-tubulin, β-tubulin mutants, and β-tubulin/ftsZ chimeras, we assessed the contribution of select regions of β-tubulin to CCT binding. In a complementary study, we investigated inter-ring communication in CCT where we exploited polypeptide binding sensitivity to nucleotide to quantitate nucleotide binding. β-Tubulin bound with a high apparent affinity to CCT in the absence of nucleotide (apparent $K_D \sim 3$ nM; its apparent binding free energy, ΔG, ca. −11.8 kcal/mol). Despite this, the interactions appear to be weak and distributed throughout much of the sequence, although certain sites ("hot spots") may interact somewhat more strongly with CCT. Globally averaged over the β-tubulin sequence, these interactions appear to contribute ca. −9 to −11 cal/mol per residue, and to account for no more than 50−60% of the total binding free energy. We propose that a conformation change or deformation induced in CCT by substrate binding provides the missing free energy which stabilizes the binary complex. We suggest that by coupling CCT deformation with polypeptide binding, CCT avoids the need for high "intrinsic" affinities for its substrates. This strategy allows for dynamic interactions between chaperonin and bound substrate, which may facilitate folding on the interior surface of CCT in the absence of nucleotide and/or productive release of bound polypeptide into the central cavity upon subsequent MgATP binding. CCT displayed negative inter-ring cooperativity like GroEL. When ring 1 of CCT bound MgATP or β-tubulin, the affinity of ring 2 for polypeptide or nucleotide was apparently reduced ∼100-fold.

The eukaryotic cytosolic chaperonin (also called CCT, TRiC, or c-cpn) is a heteromeric complex that facilitates the folding of tubulin, actin, and a number of other newly synthesized proteins in vivo (*6*−*10*). It is composed of eight or nine related gene products arranged as two back-to-back 8-fold pseudosymmetric rings (*11*−*13*). CCT and its archaebacterial relatives, the archaeosome and the thermosome, comprise the class II chaperonins. Although class II chaperonins display only a low level of sequence homology with class I chaperonins such as GroEL, they share similar structure and function in promoting protein folding in the cell. Like GroEL, CCT binds polypeptides within its central cavity (*14*, *15*), and subsequently releases these polypeptides in a MgATP-dependent reaction (*7*, *14*). In the case of α- and β-tubulin, partial maturation is thought to occur in association with CCT (*3*, *16*). In vivo, the folding and processing of the subunits are complicated. Five cofactors process the released subunits to generate the αβ-heterodimer (*17*). In addition, a heterohexameric chaperone protein, prefoldin/GimC, which binds nascent polypeptides is thought to transfer α,β-tubulin to CCT and may have other functions as well (*18*−*20*).

Important functional differences may exist between the two classes. Unlike the class I chaperonins, the class II chaperonins do not appear to utilize GroES-like co-chaperonins. In the thermosome (*21*, *22*) and CCT (*23*), helix−turn−helix projections extending from the apical domains are thought to seal the central folding cavity much as the GroES co-chaperonin caps GroEL. Thus, in the class II chaperonins, it is possible that co-chaperonin function has been subsumed within the chaperonin itself. Inter-ring communication is essential for class I function. GroEL, for example, has been described as a two-stroke engine where the GroEL rings alternate in function: one ring loading up the reactants as the other expels the products (*24*−*27*). Here MgATP binding strengthens while hydrolysis weakens inter-

[†] This work was supported in part by ACS Grant RPG-94-002-04-CB (to H.S.).

[‡] Portions of this study were presented at the European Research Conference on the Biology of Molecular Chaperones, May 1997, and at the ASCB meeting, December 1997.

* Corresponding author. Telephone: (216) 368-3387. Fax: (216) 368-3395. E-mail: hxs3@po.cwru.edu.

[§] Case Western Reserve University.

[||] University of Medicine and Dentistry of New Jersey.

[⊥] Yale University School of Medicine.

10.1021/bi992110s CCC: $19.00
Published on Web 03/18/2000

ring communication in a coordinated manner to facilitate folding (*24*, *25*, *28*). In this process, substrate is thought to bind tightly to the chaperonin in the absence of MgATP and to be released into the central cavity upon subsequent MgATP binding or hydrolysis (*29*, *30*). Inter-ring communication may be different in the class II chaperonins. The crystal structure of the thermosome (*21*) shows the subunits organized into apical, intermediate, and equatorial domains as observed for GroEL (*31*). In both classes, MgATP binds to the equatorial domain. However, in contrast to GroEL where this binding induces a large conformation change in the apical domain, MgATP binding in CCT induces large changes in both the apical and equatorial domains (*32*). Genetic analysis further suggests that MgATP binding or hydrolysis occurs cooperatively in CCT as in GroEL but in a manner different from the concerted cooperativity proposed for GroEL (*33*).

Hydrophobic interactions, which play such a dominant role in the interaction of GroEL with substrate, may play a lesser role in the case of CCT. For example, CCT is thought to have high affinity for late-forming (quasi-native) folding intermediates of tubulin and actin. In contrast, GroEL is thought to have high affinity for both early (molten globule)- and late-forming folding intermediates of tubulin and actin, and does not mediate productive folding of these proteins (*34*, *35*). These data suggest that the mechanisms by which class I and II chaperonins fold protein may differ substantially.

To examine the folding mechanism of the class II chaperonin CCT, we previously implemented a proteolytic and mutational study of β-tubulin (*3*), which supported the notion of quasi-native chaperonin-bound β-tubulin folding intermediates (*16*). Two "domains" similar in size to the putative domains in the native protein were implicated in facilitated folding by CCT. A major CCT-interacting region, residues ~150−350, was identified that encompassed portions of the two domains and an intervening protease-sensitive region. This region, named the "interactive core", was proposed to be responsible for the high-affinity binding of β-tubulin to CCT (*3*).

In the study presented here, we used limiting amounts of β-tubulin and β-tubulin mutants and a more quantitative method to probe polypeptide binding to CCT. Surprisingly, the interactions with CCT appear to be weak and to contribute less than ~50−60% to the binding free energy. We attribute the missing free energy to a stabilizing conformational change induced in CCT by β-tubulin binding. This deformation allows dynamic interactions with bound substrate, which may have profound consequences for function. In a complementary study, we show that inter-ring communication in CCT is regulated by MgATP binding and hydrolysis in a manner apparently similar to that in GroEL.

EXPERIMENTAL PROCEDURES

Site-Directed Mutagenesis. "Altered Sites II" (Promega) was used to mutagenize plasmid pALTER/β (*3*) and pALTER/Ac, which encode the chicken βII-tubulin and human skeletal muscle α-actin sequences, respectively. Codons for hydrophobic (pALTERβ41) or hydrophobic and charged amino acid (pALTERβ42) residues in the region of residues 259−272 of chicken βII-tubulin were replaced with codons for alanyl residues, and the entire β-tubulin sequence was subcloned into the overexpression vector pET28a (Stratagene) for production of Mut. 1 and 2, respectively. To produce Mut. 3, a mutant in which hydrophobic residues in the region of residues 310−318 in β-tubulin were replaced with alanyl residues, pET11Cβ8 (*3*) was altered by PCR using the "Quik-Change" method (Stratagene). Vectors for N-terminal fragments were generated by the introduction of stop codons after residue 144, 203, or 249 in pET11Cβ8.

Construction of β-Tubulin/FtsZ Chimeras. Chimeras were constructed from pET11Cβ8, which encodes chicken βII-tubulin, and from pET21AftsZ, which expresses the *Escherichia coli* ftsZ protein. To facilitate selection of the fusion points, the *E. coli* ftsZ protein sequence was mapped onto the *Methanococcus jannaschii* ftsZ protein sequence by means of the sequence alignment program of DNAStar. Gene splicing by overlap extension (*36*) was used to generate the following paired chimeras: β**1**−**203**/ftsZ164−383 (F1) and ftsZ1−163/β**203**−**445** (F2), β**1**−**218**/ftsZ174−383 (F3) and ftsZ1−173/β**219**−**445** (F4), and β**1**−**243**/ftsZ204−383 (F5) and ftsZ1−204/β**245**−**445** (F6).

In Vitro Transcription and Translation. pET plasmids were linearized with appropriate restriction enzymes and transcribed with T7 RNA polymerase. mRNAs were translated in nuclease-treated rabbit reticulocyte lysate (RRL) in the presence of [^{35}S]methionine.

Preparation of Denatured Protein. pET plasmids in *E. coli* BL21(DE3)pLysS were induced with IPTG in the presence of [^{35}S]methionine, and the overexpressed products were purified from inclusion bodies as described previously (*3*, *14*).

Alignment of the β-Tubulin Sequence on the Actin Sequence. The Needleman and Wunsch algorithm (*4*) was used with a 35-residue window (Look Program) to align the chicken β-tubulin sequence on the human skeletal (hSK) actin sequence. Four regions with a low degree of homology were revealed: β-tub 71−105 with hSK 55−90, β-tub 141−175 with hSK 143−175, β-tub 251−287 (HR2) with hSK 246−283 (the "hydrophobic plug"), and β-tub 326−360 with hSK 322−356.

Chaperonin Binding Reactions with Newly Synthesized Protein. Wild-type or mutant mRNAs were translated in RRL in the presence of [^{35}S]methionine at 30 °C for 8 min and chased in the presence of 1 mM methionine for 6 min. Aliquots (2 μL) of the translation reaction mixtures were added to tubes containing RRL diluted in RRL dilution buffer [15 mM HEPES/KOH (pH 7.5), 80 mM KOAc, 0.5 mM $Mg(OAc)_2$, 20 nM hemin hydrochloride, 2 mM DTT, 1 mM ATP, 0.4 mM GTP, and 10 pg/μL pepstatin, leupeptin, and aprotinin] to final chaperonin concentrations ranging from 4 to 200 nM (100 μL final volume). RRL is 200 nM in CCT (*8*). Samples were supplemented with 15 mM EDTA and incubated for 10 min at 30 °C. The binding reaction mixtures were chromatographed on a Superose 6 size-exclusion column (Pharmacia) at 4 °C in 150 mM KCl, 2 mM $MgCl_2$, and 20 mM sodium phosphate (pH 7.0) at a flow rate of 0.4 mL/min. Fractions (200 μL) were collected.

Chaperonin Binding Reactions with Urea-Denatured Protein. CCT was purified from bovine testis as previously described (*8*). GroEL was obtained from Epicenter Technologies. The chaperonin concentration was varied by diluting into folding buffer [20 mM MES (pH 6.8), 100 mM

KCl, 2 mM $MgCl_2$, 1 mM EGTA, 1 mM DTT, 1 mM ATP, and 0.4 mM GTP] (*37*). Overexpressed protein in 7.5 M urea was diluted 100-fold (final [^{35}S-labeled substrate] = 0.8−1.5 nM) into purified CCT preparations at concentrations typically ranging from 4 to 200 nM. Higher concentrations of CCT (up to 2 μM) were used in some studies. Binding reaction mixtures were incubated at 30 °C for 3 min, supplemented with 15 mM EDTA, and incubated for an additional 7 min. Samples were supplemented with BSA (10 mg/mL final concentration) prior to chromatography on the size-exclusion column to reduce nonspecific losses of free folding intermediates on the column. In some studies, RRL was used as the source of CCT. Binding studies were carried out as described above except that RRL dilution buffer was used instead of folding buffer and no carrier protein was added.

In studies with nucleotide carried out under conditions that permit MgATP binding or hydrolysis, folding buffers were supplemented with Mg^{2+} and ATP as required (EDTA was not used in these studies). Incubation times were also increased as indicated. To assess binding affinities, in some studies samples were chromatographed on the size-exclusion column with running buffers supplemented with nucleotide and $MgCl_2$ to final levels identical to those during incubations in folding buffer.

Analysis of Binding Data. Binding studies were performed under substrate-limiting conditions ($[CCT]_{total} \gg [\beta\text{-tubulin}]_{total}$). Total counts per minute (cpm) recovered ("TCR") from the size-exclusion column, taken as the sum of scintillation counts in fractions 30−100, were monitored in the urea-denatured studies and decreased with CCT dilution, typically by ∼1−2-fold between the most concentrated and the least concentrated samples. These differences presumably reflected an increased level of substrate loss (free intermediate) and resulted in a slight underestimation of the K_D. Differences in ΔG ($\Delta\Delta G$), which involve a ratio of apparent K_D values, were relatively insensitive to these losses. Chromatograms were renormalized to yield the same TCR value. Fraction of substrate bound to CCT or GroEL was calculated by dividing the cpm sum of fractions eluting at the chaperonin positions by the cpm sum of fractions eluting at the chaperonin and free folding intermediate ("I") positions, and least-squares fitted (with MacCurveFit) to eq 1 to obtain the apparent K_D.

$$\text{fraction substrate bound} = \frac{[\text{chaperonin}]_{free}}{K_D + [\text{chaperonin}]_{free}} \quad (1)$$

In cases where the binding studies were repeated two or more times ($n > 1$), the listed K_Ds (Tables 1 and 2) represent the average K_D value ± the standard deviation (SD). SD values reported for single determinations ($n = 1$), on the other hand, reflect the goodness of fit to eq 1. Under our substrate-limiting conditions, $[\text{chaperonin}]_{free} \sim [\text{chaperonin}]_{total}$. To assess CCT stability during dilution, we prepared [^{35}S]CCT by exchange of newly synthesized [^{35}S]TCP1α into CCT (*38*) and determined the amount of intact CCT recovered from the column for various diluted initial samples. The data indicated that CCT is stable to at least 4 nM (data not shown).

The N-terminal fragment studies were characterized by extensive loss of the free intermediate (Figure 3). For each set of chromatograms in a dilution study, self-consistent estimates of the fraction bound were obtained by iterative fits of the cpm eluting at the chaperonin position to eq 1 (assuming an initial value of 1 for the fraction bound at the highest chaperonin concentration). For mutants Δ2−145, Δ85−144, Δ86−251, and Δ85−306 (Figure 9), apparent K_Ds and ΔGs were estimated from single concentration studies at 200 nM CCT (data from Dobrzynski et al.). The fraction bound was determined from SDS−PAGE fluorographs of column fractions (data not shown).

Binding studies were also carried out with urea-denatured wild-type β-tubulin under conditions where ring 1 is occupied with MgATP ([MgATP] > 0.04 mM) (*14*). Apparent K_Ds for β-tubulin bound to ring 2 were estimated from eq 1 and fitted to eq 2 to obtain $K_{D,Nuc2}$, the apparent dissociation constant of MgATP for ring 2. Equation 2 is derived from eq 1 when $[CCT]_{total} > 100$ nM and $[MgATP]/K_{D,Nuc2} < 20$ (conditions satisfying $[CCT]_{free} > [\beta\text{-tubulin}]_{total}$), and takes into account saturation of ring 2 with MgATP. We assume that

$$K_{D,app} = K_{D,ave} + \frac{K_{D,ave}[MgATP]}{K_{D,Nuc2}} \quad (2)$$

CCT with MgATP in rings 1 and 2 does not bind polypeptide. $K_{D,ave}$ is the average value (∼20 nM) for K_D in the MgATP concentration range of 0.2−4 mM, where CCT is essentially free of MgATP in ring 2 (Results). The MgATP-dependent term is a correction for saturation, where binding of β-tubulin is only to residual chaperonins free of nucleotide in ring 2. When $0.2 \leq [MgATP] \leq 4$ mM, K_Ds were estimated from dilution studies. In the saturation range ([MgATP] > 4 mM), apparent K_Ds were estimated from single-CCT concentration studies except where noted. Equation 2 does not take into account cooperativity. Consequently, it fits the high-MgATP concentration data well and gives only "average" K_D values at low MgATP concentrations where nucleotide binding is complex and cooperativity is important (Figure 7C).

The relationship $\Delta G = RT \ln K_D$ was used to estimate the apparent binding free energy. We used the "average contribution per β-tubulin residue" to ΔG as a convenient measure of the level of interaction of β-tubulin regions with CCT and distinguished between locally and globally averaged contributions. The globally averaged contribution per residue is defined as the ΔG of the binding reaction divided by the number of β-tubulin residues in the polypeptide. Globally averaged contributions were either inferred from plots of the ΔGs (Figure 9) or calculated (Table 3, text).

RESULTS

Polypeptide Binding Studies

Role of Hydrophobic Sites in β-Tubulin Binding to CCT. Residues ∼150−350 of β-tubulin were previously identified as the primary region of interaction with CCT ("interactive core", Figure 1A) (*3*). This region contains the intermediate ("M") domain (residues ∼205−384) of native β-tubulin (*39*). Since hydrophobic residues play a key role in substrate binding to GroEL, the contribution of hydrophobic sites within β-tubulin to CCT binding was investigated. Hydrophobicity plots (*40*) show three hydrophobic regions in the M domain: residues 225−240 (HR1), 259−278 (HR2), and

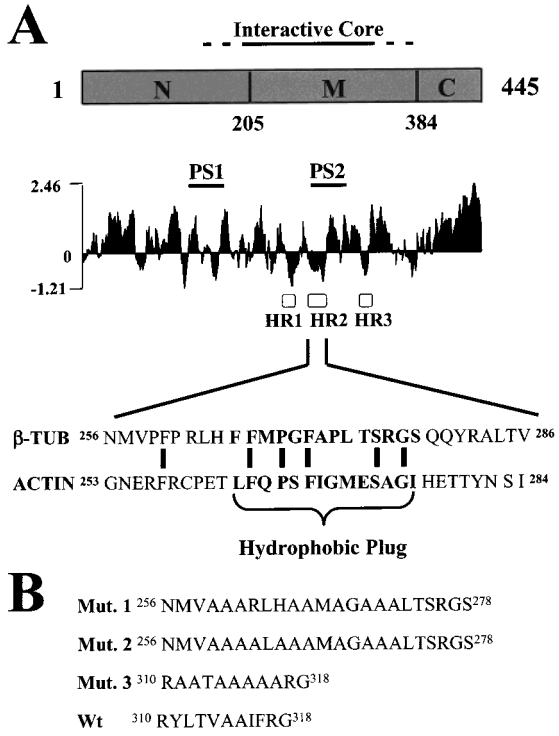

FIGURE 1: Hydrophobic regions of β-tubulin. (A) The β-tubulin amino acid sequence was assessed for hydrophobic segments by the Kyte−Doolittle method using the Protean program by Lasergene. PS1 and PS2 denote the two protease-sensitive regions of the native protein. Three hydrophobic regions were identified within the interactive core: HR1 (residues 227−241), HR2 (residues 259−272), and HR3 (residues 309−318). The amino acid sequence for HR2 is shown aligned with a region with a low degree of sequence homology in actin that includes the hydrophobic plug (shown in bold). (B) Hydrophobic residues in HR2 (Mut. 1) and HR3 (Mut. 3) were mutated to alanines as indicated. Hydrophobic *and* charged residues in HR2 were mutated to alanines in Mut. 2.

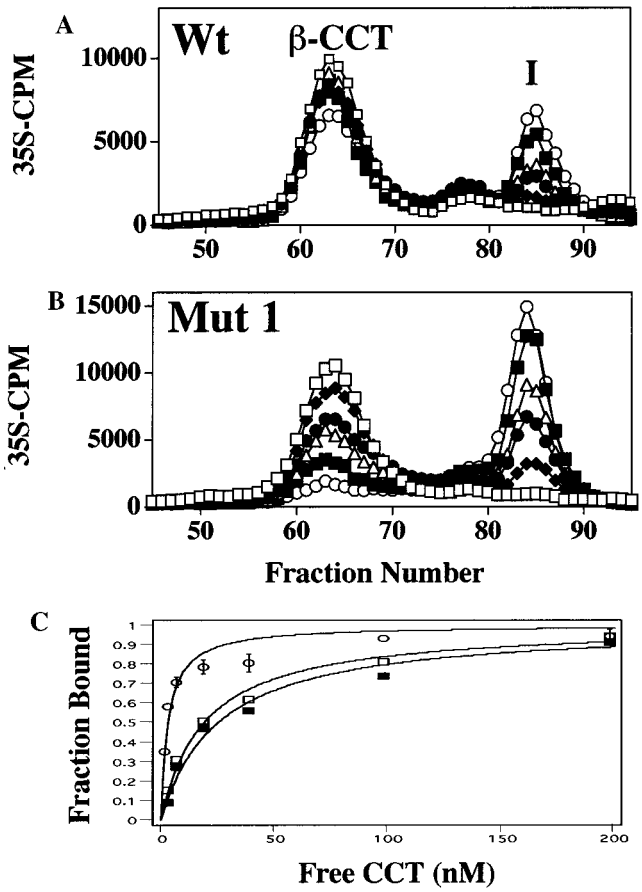

FIGURE 2: Mutation of the region of residues 259−272 reduces the affinity for CCT by ~8−10-fold. (A) Binding of urea-denatured wild-type β-tubulin. Urea-denatured wild-type [^{35}S]-β-tubulin was diluted into RRL containing 200 (□), 100 (◆), 40 (●), 20 (△), 8 (■), 4 (○), and 2 nM CCT (not shown) and incubated and processed as described in Experimental Procedures. Binding reaction mixtures were chromatographed on a Superose 6 column at 4 °C. β-tub-CCT and I denote the elution positions of the CCT−β-tubulin binary complex and the free β-tubulin folding intermediate, respectively. (B) Binding of urea-denatured Mut. 1. Binding was assessed as described for panel B. Chromatograms for Mut. 1 are shown (plot symbols are identical to those in panel B). Similar chromatograms were obtained for Mut. 2 (data not shown). (C) The fractions of the wild type (○), Mut. 1 (□), and Mut. 2 (■) bound as a function of CCT concentration. Bound fractions were determined and fitted by least-squares analysis to eq 1. Renormalization factors for the chromatograms ranged from 1 to 1.7 for the wild type and from 1 to 1.4 for Mut. 1 (Experimental Procedures).

310−318 (HR3) (Figure 1A). In native β-tubulin, residues 265−278 of HR2 form β-strand S7 and part of the M loop responsible for lateral protofilament interactions in the microtubule. HR3 comprises a β-strand, S8, which lies in the same sheet as S7, and HR1 encompasses mainly the "core helix", a structurally important element that packs against the N and M domains (*39*, *41*) (Figure 4A below). It was previously suggested that CCT recognizes sites important for protein−protein interactions and/or self-assembly and that HR2 plays a major role in these interactions (*3*). To estimate the contributions of HR2 and HR3 to binding, the hydrophobic residues of HR2 (Mut. 1) and HR3 (Mut. 3) or hydrophobic and charged residues of HR2 (Mut. 2) were replaced with alanyl residues (Figure 1B). N-Terminal fragments 1−203 and 1−250, which bracketed HR1, were used to estimate the contribution of HR1. Binding was assessed in the presence of EDTA with urea-denatured protein and, in select cases, with newly synthesized polypeptides in RRL. Similar affinities were obtained with urea-denatured and newly synthesized proteins (Table 1). EDTA prevents MgATP binding or hydrolysis by the chaperonin and, therefore, processing of β-tubulin in RRL. Control studies with wild-type and purified CCT in the absence of nucleotide gave essentially the same K_D (~3 nM) as that obtained with nucleotide and EDTA (Table 1). In the study whose results are depicted in Figure 2, wild-type [^{35}S]-β-tubulin or mutants overexpressed in *E. coli* were diluted out of urea and incubated with various dilutions of RRL containing final CCT concentrations ranging from 2 to 200 nM prior to elution on a size-exclusion column. Radiolabeled protein eluted mainly at two positions, an early-eluting peak (fractions 58−69), which corresponds to a CCT-associated form of β-tubulin ("β-tub-CCT"), and a later-eluting peak (fractions 80−90), which contains the CCT-free β-tubulin folding intermediate ("I"). A comparison of chromatograms indicated that the HR2 mutants, Mut. 1 (Figure 2B) and Mut. 2 (not shown), have significantly reduced affinities for CCT relative to the wild type (Figure 2A). Least-squares analysis of the data (Figure 2C) indicated an apparent K_D value of 2.8 ± 0.3 nM for the wild type and 8−10-fold higher apparent K_D values for the HR2 mutants (Table 1), which translate to binding free energies (ΔG) of −11.8 and −10.5 kcal/mol, respectively. In contrast, replacement of hydrophobic residues in HR3 with alanyl residues had no effect

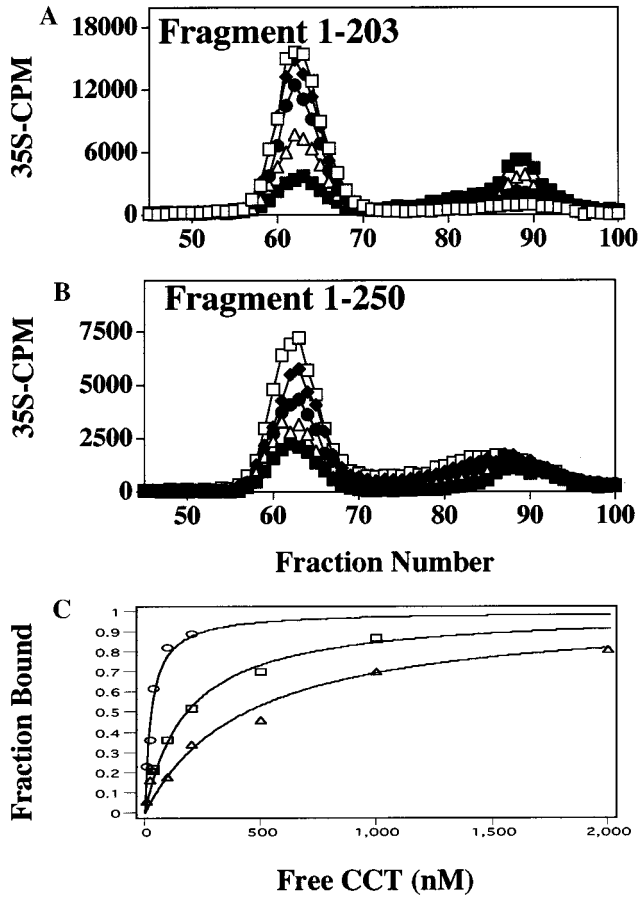

FIGURE 3: Contribution from residues 203−250. (A) Binding of the urea-denatured N-terminal fragment 1−203. The ^{35}S-labeled fragment 1−203 was diluted out of urea into solutions containing 1000 (□), 500 (◆), 200 (●), 100 (△), and 40 nM purified CCT (■) and processed as described in the legend of Figure 2. (B) Binding of the urea-denatured N-terminal fragment 1−250. The urea-denatured ^{35}S-labeled fragment 1−250 was diluted into folding buffer containing 200 (□), 100 (◆), 40 (●), 20 (△), and 8 nM purified CCT (■) and processed as described for panel A. Note the extensive loss of the free folding intermediates (fractions 80−93) in panels A and B. (C) The fraction bound as a function of CCT concentration: residues 1−250 (○), 1−203 (□), and 1−144 (△) (chromatograms not shown). Bound fractions were estimated and fitted by least-squares analysis as described in Experimental Procedures.

on affinity. Deletion of residues 203−250 apparently had a small effect on binding affinity as indicated by a 5−6-fold estimated increase in the K_D value of the N-terminal fragment 1−203 relative to that of 1−250 (Table 1 and Figure 3). The data imply that HR1 and HR2 together increase binding affinity by 30−50-fold. This translates to an apparent contribution to ΔG of ca. −2 kcal/mol from residues ∼204−280. HR2 is an apparent "hot spot" which contributes −1.4 of this −2 kcal/mol.[1] Taking all the results together, we conclude that HR1, HR2, and HR3 apparently contribute no more than 15−20% to the total ΔG. Residues 265−278 of HR2 are ∼30% homologous with residues 263−276 of actin (Figure 1A), which form a loop or hydrophobic plug thought to stabilize lateral interactions in F-actin (*42*). In contrast to HR2, mutation of the homologous region in actin had no effect on actin's affinity for CCT (Table 1). This finding is consistent with a recent study of actin binding to CCT (*2*) and does not support the hypothesis that these hydrophobic loops of actin and tubulin define a general recognition motif for the chaperonin (*3*). Table 1 lists the apparent K_D values for substrates bound to ring 1 of CCT in the absence of nucleotide. We also list, for purposes of comparison, the apparent K_D value for wild-type β-tubulin in the *presence* of 0.5 mM MgATP. This value is ∼6−8-fold larger than the apparent K_D value for wild-type β-tubulin in the absence of nucleotide and reflects binding of β-tubulin to ring 2 when ring 1 is saturated with MgATP (and therefore incapable of binding polypeptide) (Figure 7C inset, below).

β-Tubulin/FtsZ Chimera Proteins (CCT versus GroEL). We were concerned that the truncations and the alanine substitutions may have grossly perturbed the conformation of the folding intermediates, causing artifactual results. In an effort to overcome these concerns, we generated chimeric proteins of β-tubulin and its structural relative, the *E. coli* protein ftsZ.

FtsZ is the major cytoskeletal protein in bacterial cell division. Like tubulin, ftsZ binds and hydrolyzes GTP and self-assembles into higher-order structures (*43*). The structures of *M. jannaschii* ftsZ and bovine β-tubulin are strikingly similar, but their sequences are only 13% homologous (Figure 4A) (*39*, *44*). They are composed of two similar principal domains, each comprised of a β-sheet surrounded by α-helices, folded against a core helix (Figure 4A). Six chimeric proteins were generated using PCR-based gene splicing (Experimental Procedures). The chimeras were designed so the domain structure of their component parts could be maintained. Thus, the linkage site was either at the terminal β-strand of "domain" 1 of ftsZ or β-tubulin (F1 and F2) or immediately preceding (F3 and F4) or immediately following (F5 and F6) the core helix in each protein (*39*, *44*) (Figure 4B).

Wild-type β-tubulin, wild-type ftsZ, and the N- and C-terminal β-tubulin chimeras were assessed in binding studies with CCT purified from bovine testis. The apparent K_D values are reported in Table 2 with select chromatograms shown in Figure 5. When expressed in RRL, ftsZ is not co-immunoprecipitated by antibody 23C, which recognizes TCP-1α and co-immunoprecipitates tubulin and actin (data not shown). Consistent with this result, CCT gave a K_D of >10000 nM for ftsZ (Figure 5A). In addition, ftsZ did not associate with the bacterial chaperonin, GroEL (Figure 5A). The chimeras displayed a range of affinities for CCT as observed with the β-tubulin fragments, confirming that the CCT-binding sites in β-tubulin are present in both domains of the protein. The apparent K_D for fragment 1−250 differed by a factor of ∼5−6 from that of **β1−243**/ftsZ204−383, which may reflect a somewhat perturbed conformation in the folding intermediate of residues 1−250. Apparent K_Ds for the N-terminal chimeras were similar to or slightly higher than those for the C-terminal chimeras. The sum of the binding free energies of the paired chimeras is remarkably

[1] We have found the "average contribution per β-tubulin residue" to ΔG a convenient measure of the level of interaction of β-tubulin regions with CCT (Experimental Procedures). Apparently, residues 260−280 of HR2 contribute on the average ca. −140 cal mol^{-1} residue^{-1} to ΔG. This contrasts with that of residues 203−250 where each residue apparently contributes on the average ca. −19 cal mol^{-1} residue^{-1} to ΔG, a value not substantially different from the *globally averaged* estimated contribution of ca. −27 cal mol^{-1} residue^{-1} for the wild-type protein (−12 kcal/mol per 445 residues) uncorrected for a possible conformation change in CCT, or from the ca. −10 cal mol^{-1} residue^{-1} corrected (see the Discussion).

Table 1: Apparent CCT Dissociation Constants for β-Tubulin and Actin Polypeptides

	K_D (nM)		
	I[a]	II[b]	III[c]
β-tubulin			
wild type	2.8 ± 0.3	4.5 ± 0.6 (n = 2)	2.5 ± 0.2
with 0.5 mM MgATP[d]		26 ± 4 (n = 4)	
HR2			
Mut. 1	20 ± 1.4	35 ± 8	19 ± 3.3
Mut. 2	26 ± 2.7		31 ± 6.3
HR3			
Mut. 3	3.3 ± 0.4	6.9 ± 2.5	
HR1			
residues 1−203		160 ± 20	210 ± 20 (n = 2)
residues 1−250		28 ± 2	
actin			
wild type	13 ± 4.0 (n = 3)		
Mut. A[e]	12 ± 2.0 (n = 2)		

[a] Urea-denatured into RRL. [b] Urea-denatured into purified CCT. [c] Binding reactions with newly synthesized protein (see Experimental Procedures). [d] See the inset of Figure 7C. [e] Mut. A, ^{260}AQPAAAGAAS^{271}; wild type, ^{260}FQPSFIGMES^{271}.

constant at −18.7 ± 0.1 kcal/mol (Table 3, column 2). This result supports the notion that the overall conformation and/or domain structures of the chimeras were not significantly different from intact β-tubulin and ftsZ.

The chimera results follow a consistent pattern. There appear to be no single or multiple regions within the interactive core that can account for the high-affinity binding of β-tubulin to CCT. The apparent K_Ds (Table 2, CCT data) show a 2 order of magnitude range, i.e., a spread of ca. −2 to −2.5 kcal/mol in apparent ΔG values. This spread is relatively insignificant compared with the total binding free energy of ca. −11.8 kcal/mol for the intact protein. This surprising and paradoxical result, we believe, has important implications (Discussion).

Binding studies were also performed with GroEL to elucidate the functional differences between the chaperonins (Figure 5 and Table 2). Intact β-tubulin bound tightly to GroEL, with a K_D that was ∼2-fold higher than that for CCT (Table 2). C-Terminal chimeras also bound tightly to GroEL. In contrast, N-terminal chimeras bound weakly to GroEL (K_D > 4 μM). These results suggest that GroEL binds the M and C but not the N portions of the intact protein. GroEL also binds Mut. 1 and 3 and the wild type with similar affinities (Table 2) and thus appears not to interact with residues 259−272 or with residues 310−320.

Taken together, the results suggest that GroEL may not interact with residues N-terminal to residue 320. This is surprising since the major hydrophobic regions in β-tubulin are N-terminal to this residue. These results likely indicate different interactions of β-tubulin with the apical domains of the chaperonins. However, since CCT is larger than GroEL, an alternative explanation is that physical constraints limit the insertion of β-tubulin into GroEL, and it is mostly the C-terminal portion that is accommodated within the channel. This possibility is supported by the observation that the N-terminal fragments interact with GroEL (K_D ∼ 100 nM) (Table 2).

Chymotryptic Digestion Studies of the Folding Intermediate. To compare the folded state of bound and free folding

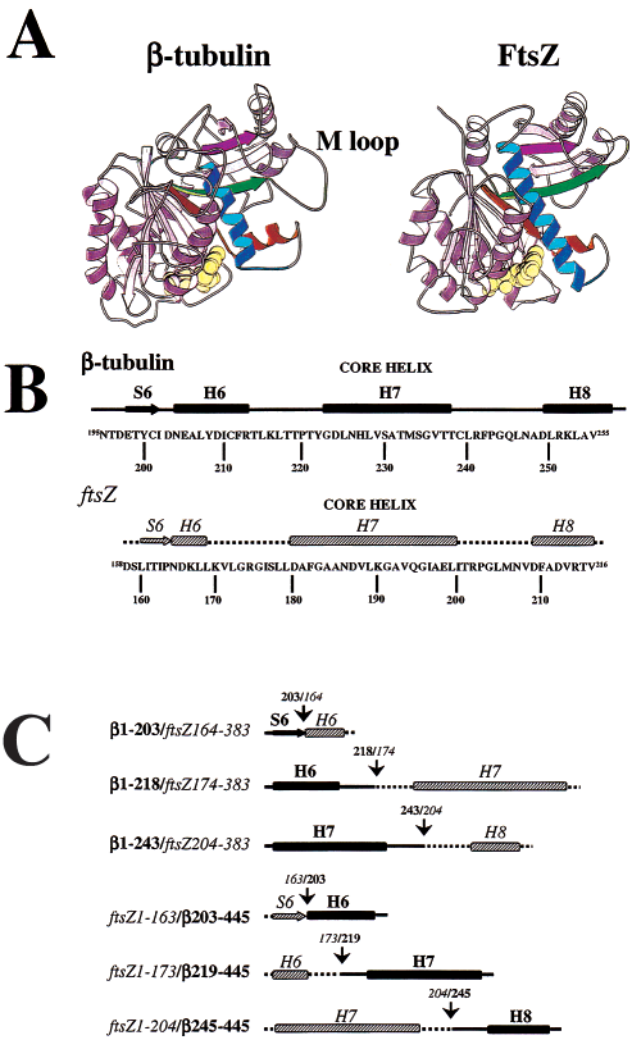

FIGURE 4: β-Tubulin/ftsZ chimera constructs. (A) Ribbon diagrams of ftsZ and the β-tubulin subunit. The latter is extracted from the structure of the native tubulin heterodimer (*39*). Native β-tubulin folds into an N-domain (residues 1−205), an M-domain (residues 205−384), and a C-domain (residues 385−445). The S6 strand (residues 198−202) and the H6 helix (residues 205−213) of β-tubulin are colored brown; the core helix (H7) is blue, and the S8 strand is magenta. The same color scheme is used for ftsZ. The protease-sensitive region of residues ∼260−290 (*1*) (green) encompasses HR2 and a portion of the "M" loop. Note the small "M" loop in ftsZ. The GTP moiety is yellow. (B) Secondary structure elements and amino acid sequences of ftsZ and the β-tubulin subunit are shown relative to their core helices (bar = helix; arrow = β-strand). (C) Fusion regions of β-tubulin/ftsZ chimeras. Three N-terminal and three C-terminal chimeras were constructed (proceeding top to bottom, chimera proteins F1, F3, F5 and F2, F4, and F6, respectively). Lines, arrows, and bars that are solid represent β-tubulin secondary structural elements. Dotted lines, hatched arrows, and hatched bars represent ftsZ elements. Vertical arrows denote the fusion points.

intermediates, wild-type intermediate "I" was tested for sensitivity to chymotrypsin and for its ability to reassociate with CCT (Figure 6). When [^{35}S]-β-tubulin was diluted out of urea into 4 nM CCT, ∼40% of the radiolabel eluted at position "I". As expected, when an aliquot was incubated with 200 nM CCT, radiolabeled "I" reassociated quantitatively with CCT (Figure 6A). Since "I" is non-native, it should also be more sensitive to chymotrypsin than the "mature" native-like form of β-tubulin released from CCT (*3*). Non-native "I" isolated from a 4 nM binding reaction

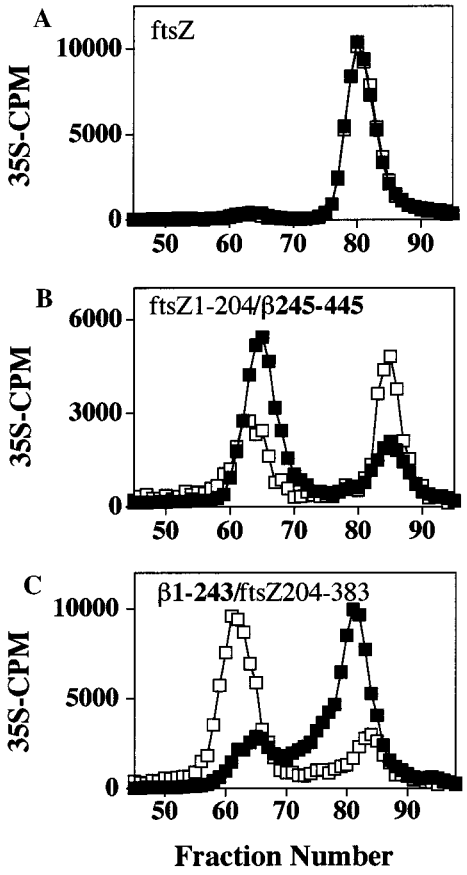

FIGURE 5: Interaction of β-tubulin/ftsZ chimeras with CCT and GroEL. (A) FtsZ does not bind CCT or GroEL. [^{35}S]FtsZ was diluted out of urea into 1 μM purified CCT (□) or 1 μM GroEL (■). Samples were incubated and processed as described in the legend of Figure 2 except that BSA was added as a carrier protein prior to chromatography. (B and C) Binding chromatograms for ftsZ1−204/β**245**−**445** (F6) and β**1**−**243**/ftsZ204−383 (F5). CCT binds with a similar affinity to the N- and C-terminal chimeras with K_Ds ranging from 100 to 300 nM (Table 2). (B) C-Terminal chimeras bind with a high affinity to GroEL. C-Terminal chimeras were diluted from urea into solutions containing 200 nM GroEL (■) or 200 nM purified CCT (□) and processed as described for panel A (only F6 chromatograms are shown). The apparent K_D for F6 and GroEL is ~38 nM. (C) N-Terminal chimeras bind with a low affinity to GroEL. N-Terminal chimeras were diluted from urea into solutions containing 2 μM GroEL (■) or 500 nM purified CCT (□) and processed as described for panel A (only F5 chromatograms are shown). The apparent K_D for F5 and GroEL is >10 μM. In contrast, the N-terminal fragments display intermediate affinities for GroEL. This may reflect unmasked site(s) or possibly differences in substrate accessibility. Note the three- to four-fraction shift in the peak position of the GroEL relative to the CCT. This reflects the smaller size of GroEL.

in RRL (with EDTA) was subjected to limited digestion with chymotrypsin on ice. For comparison, β-tub-CCT isolated from a 200 nM CCT binding reaction mixture was adjusted to a final CCT concentration of 10, 50, or 200 nM and similarly digested. The loss of full-length protein exhibited biphasic kinetics. Proteolytic conditions that produced modest levels of digestion of the "partially mature", nearly native monomer (*3*, *7*) caused extensive digestion of "I". More than 98% of "I" was digested within 30 s of the addition of chymotrypsin (Figure 6B,C). The remaining 1−2% of full-length "I" digested slowly. Binding partially protects the intermediate. Sixty to seventy percent of the bound form was digested within 1 min of protease addition; an additional 5−10% of full-length protein was digested by 10 min (Figure 6B,C). Fragmentation patterns of β-tubulin−CCT are similar to that reported for a similar nucleotide-free study by Dobrzynski et al. but differed in intensities from that observed in the presence of nucleotide (*3*).

Table 2: Apparent Dissociation Constants for β-Tubulin Fragments, Chimera Proteins, and Mutants[a]

	K_D (nM)	
	CCT	GroEL
wild-type β-tubulin	4.5 ± 0.6 (n = 2)	8.1 ± 0.3 (n = 3)
wild-type ftsZ	>10000[b] (n = 2)	>10000 (n = 2)
N-terminal fragments		
1−144	435 ± 70	ND
1−203	160 ± 20	90 ± 11
1−250	28 ± 2	72 ± 8
N-terminal chimeras		
β**1**−**203**/ftsZ164−383	289 ± 29[b]	>4000 (n = 2)
β**1**−**218**/ftsZ174−383	248 ± 28[b]	>4000
β**1**−**243**/ftsZ204−383	148 ± 23[b]	>4000 (n = 2)
C-terminal chimeras		
ftsZ1−163/β**203**−**445**	107 ± 28	21 ± 4 (n = 2)
ftsZ1−173/β**219**−**445**	87 ± 11	8.5 ± 3.0 (n = 2)
ftsZ1−204/β**245**−**445**	204 ± 36	38 ± 13
Mut. 1	35 ± 8	1.3 ± 0.7
Mut. 3	6.9 ± 2.5	3.0 ± 0.4 (n = 2)

[a] Studies performed with purified chaperonin. [b] Similar values also obtained using RRL.

Digestion rates and fragmentation patterns of *full-length* β-tubulin complexed to CCT were *independent* of chaperonin concentration over a 20-fold range ($2K_D$ < [CCT] < $50K_D$) (Figure 6B). This indicated a tight association of polypeptide with CCT and did not support the possibility that free "I", either in equilibrium with CCT or exchanging with bound "I", affected the digestions. This conclusion is supported by a previous report by Farr et al. (*8*), who found that wild-type β-tubulin folding intermediates bind tightly to CCT in the absence of nucleotide and apparently have very low rates of dissociation as these intermediates cannot be readily captured by GroEL traps. Surprisingly, fragmentation patterns of the bound and free β-tubulin were remarkably similar (Figure 6B). Fragments N_t and C_t and the highly resistant 18 kDa fragment (∗) previously seen with newly synthesized CCT-bound wild-type β-tubulin were also generated from the free folding intermediate. Thus, binding to CCT *decreases the rate by which tubulin is digested without masking major cleavage sites*. Fragments N_t and C_t were attributed previously by Dobrzynski et al. to cleavage within a protease-sensitive region, residues ~260−290 (Figure 1A). This region, which encompasses HR2, coincides with strand S7 and the M loop in the native protein (Figure 4A). In RRL and in the presence of nucleotide, this strand−loop region apparently becomes increasingly resistant to protease as the β-tubulin folding intermediate matures in association with CCT (*3*).

Nucleotide Studies

GroEL displays a nested cooperativity in MgATP binding (*45*) where (I) MgATP binds cooperatively within one GroEL ring, inducing a conformational change that inhibits polypeptide binding to this ring, and (II) MgATP binding within one ring (ring 1) inhibits MgATP binding to the second ring (ring 2). Nested cooperativity is presumed to occur with CCT,

Table 3: Apparent Free Energy Changes for Binding of β-Tubulin/FtsZ Chimera Proteins to CCT[a]

paired chimeras[b]	(1) ΔG (kcal/mol)	(2) ΔG_{N+C} (kcal/mol)[c]	(3) $\Delta G_{N+C} - \Delta G_{WT}$ (kcal/mol)	(4) globally averaged contribution per tubulin residue, corrected[d] [kcal mol^{-1} (β-tubulin residue)$^{-1}$]
F1 (N1−203)	−9.0	−18.6	−6.9	−0.010
F2 (C203−445)	−9.6			−0.011
F3 (N1−218)	−9.1	−18.8	−7.1	−0.009
F4 (C219−445)	−9.7			−0.011
F5 (N1−245)	−9.4	−18.6	−6.9	−0.010
F6 (C245−445)	−9.2			−0.012
				avg −0.011 ± 0.002

[a] $\Delta G = RT \ln K_D$ (data from Table 2). [b] β-Tubulin segment in parentheses. [c] Sum of paired chimeras. [d] (Column 1 − column 3)/(number of β-tubulin residues) (Discussion). For the wild type, (−11.8 kcal/mol − column 3_{ave})/445 = −0.010 kcal mol^{-1} residue^{-1}.

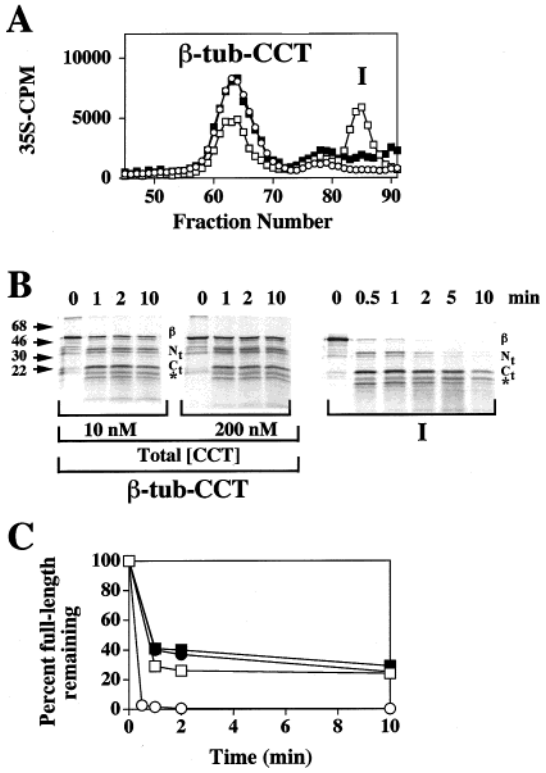

FIGURE 6: Folding intermediate "I" and β-tub-CCT are conformationally similar. (A) "I" rebinds CCT. [^{35}S]-β-Tubulin was diluted from urea into 4 (□) and 200 nM CCT (○) in RRL, and incubated and processed as described in the legend of Figure 2. Prior to chromatography, samples were supplemented with BSA as a carrier protein. A 20 μL aliquot of the 4 nM CCT binding reaction was removed and added to 80 μL of RRL (200 nM CCT) and incubated for an additional 10 min prior to chromatography (■). More than 85% of "I" rebound CCT (97% predicted from the apparent K_D). (B) β-tub-CCT and "I" display similar chymotrypsin digestion patterns. "I" isolated from a 4 nM CCT binding reaction mixture was digested with 6 μg/mL chymotrypsin on ice for 0, 0.5, 1, 2, 5, and 10 min. [^{35}S]-β-tub-CCT, isolated from a 200 nM CCT binding reaction mixture in RRL, was adjusted to CCT concentrations of 10 and 200 nM, by dilution with buffer or by supplementation with exogenous CCT (10 min at 30 °C), and similarly digested with chymotrypsin. Digests were examined by SDS−PAGE and quantitated by PhosphorImager analysis. β denotes the full-length polypeptide, N_t the N-terminal (34−37 kDa) fragments, C_t the C-terminal (22 kDa) fragment, and ∗ a highly resistant 18 kDa fragment. (C) The percent remaining of full-length β-tubulin following chymotrypsin digestion: "I" (○) and 10 (□), 50 (●), and 200 nM total CCT (■).

although to the best of our knowledge this has not been demonstrated in the literature. EM studies of CCT show asymmetric forms in the presence of MgATP, consistent with a negative inter-ring cooperativity (*32*). However, these studies also show a pronounced tilt of the equatorial domains of the MgATP-bound ring toward the intermediate domains which reduces contact between the rings, and suggests that ATP binding or hydrolysis destabilizes CCT, possibly dissociating these chaperonins into single-ring intermediates and/or subunits during the polypeptide-folding cycle (*38*). Roobol et al. (*46*) recently reported ATP-dependent disassembly of CCT in mammalian cell extracts. Consequently, CCT may not function as a two-stroke engine as has been proposed for GroEL. We exploited the sensitivity of β-tubulin−CCT binding to nucleotide to indirectly investigate the effect of nucleotide on inter-ring communication in CCT. Preliminary studies indicated that CCT was stable in the presence of MgATP (at least several millimolar), suggesting that this indirect approach should be possible. β-Tubulin is an excellent probe for these studies. Although it cycles on-and-off the chaperonin and undergoes apparent "maturation" in the presence of MgATP, it retains a high affinity for CCT and does not mature to a stable CCT-free form in the absence of cofactors. The studies below suggest that CCT functions as a two-stroke engine. If cycles of disassembly and reassembly of CCT are indeed essential for folding (*5*, *46*), our results support the notion that these cycles have more impact on how *polypeptides* are managed than on how *nucleotides* are managed by CCT (*5*) (Discussion).

Binding studies were performed with purified CCT and limiting concentrations of urea-denatured wild-type β-tubulin in folding buffer supplemented with MgATP (Figure 7). Addition of GTP (to a final concentration of 0.4 mM) did not alter the affinity of the β-tubulin folding intermediate for CCT when tested in select cases. The MgATP concentrations that were used (>0.2 mM) were sufficiently high to saturate the nucleotide binding site of ring 1 of CCT [$K_{D,Nuc1} \sim 40$ μM (*14*)]. Under these conditions, and if CCT behaves like GroEL, measurements of K_D should be measurements of the apparent affinity of ring 2 for β-tubulin. This is a reasonable assumption since EM studies suggest that the apical domains of the MgATP-bound CCT ring undergo a conformation change that inhibits polypeptide binding, as occurs with GroEL (*23*, *32*). We reasoned that if CCT behaves like GroEL, then at MgATP concentrations that are insufficient to overcome the negative cooperativity between rings, ring 2 of CCT should be free of nucleotide and affinity for β-tubulin should be high. At sufficiently high MgATP concentrations, both rings should be occupied with nucleotide and the affinity for polypeptide should be drastically reduced.

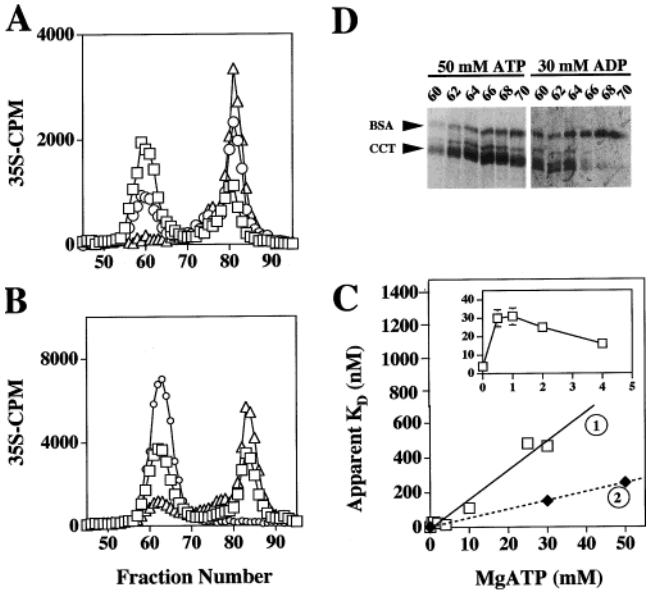

FIGURE 7: Effects of MgATP in ring 1 on β-tubulin binding to ring 2. (A) Binding to CCT at 1 mM MgATP. Purified CCT was diluted to 100 (□), 20 (○), and 2 nM (△) in buffer containing 1 mM MgATP. Urea-denatured [^{35}S]-β-tubulin was diluted into the samples and incubated for 10 min. Samples were chromatographed on a Superose 6 column. (B) Binding to CCT at high ATP concentrations. Purified CCT was diluted to 200 nM in buffer containing either 5 mM $MgCl_2$ and 10 mM ATP (□), 10 mM $MgCl_2$ and 30 mM ATP (△), or 10 mM $MgCl_2$ and 10 mM AMP-PNP (○) and incubated for 90 min. Urea-denatured [^{35}S]-β-tubulin was diluted into the samples and chromatographed as described for panel A except that running buffers were supplemented with $MgCl_2$ and ATP as in the incubations. (C) Apparent K_D vs MgATP concentration. Two independent studies were performed. In study 1, a range of ATP concentrations from 0.5 to 30 mM was examined. Purified CCT was diluted to 200 nM in buffers supplemented with 0.5, 1, 2, 4, 10, 25, and 30 mM ATP and incubated for 90 min. Folding buffer was supplemented with additional $MgCl_2$ so that ATP and $MgCl_2$ concentrations were equivalent. The 4, 10, 25, and 30 mM ATP data points fitted to eq 2 (—) gave an estimated $K_{D,Nuc2}$ value of 1.3 mM. For the 25 mM MgATP studies, binding of β-tubulin was assessed over a range of CCT concentrations (8−200 nM), whereas in the 10 and 30 mM MgATP studies, a single CCT concentration of 200 nM was used (as in panel B). Urea-denatured [^{35}S]-β-tubulin was diluted into the samples and incubated for 90 min. Samples were processed as described for panel B. Apparent K_D values (□) represent an average of at least two determinations (with the exception of the 25 mM study which was performed only once). In study 2, binding of β-tubulin to 200 nM CCT preincubated with 1, 30, and 50 mM MgATP was examined (- -◆- -). This study gave an estimated $K_{D,Nuc2}$ value of 4.4 mM. The inset is an expanded plot of the apparent K_D vs MgATP concentration. The apparent K_D displays complex behavior at low to intermediate MgATP concentrations. Note its increase from 3 nM in the absence of nucleotide to 30 nM with 0.4 mM MgATP. This increase reflects occupancy of ring 1 with MgATP and provides an upper bound estimate of <200 μM for $K_{D,Nuc1}$, consistent with the 40 μM value obtained by fluorescence (*14*). (D) Silver-stained SDS−PAGE gel of the column fractions from 50 mM ATP (left) and 30 mM ADP studies (right). Fraction numbers are indicated above the lanes. Arrows show the positions of CCT subunits and BSA (internal reference added as a carrier protein in large excess). At 50 mM MgATP, which represents the extreme end of our study, ~60% of the CCT dissociated into rings and/or oligomeric structures.

The affinity for β-tubulin was high in the presence of 1 mM MgATP (apparent $K_D \sim 28 \pm 5$ nM) (Figure 7A), although it was reduced 9−10-fold relative to those of nonnucleotide and 1 mM MgADP controls (data not shown). A drastic reduction in the apparent affinity was observed at 10 and 30 mM MgATP, concentrations that would be anticipated to result in occupation of ring 2 ATP sites (Figure 7B). At 10 mM MgATP, the apparent K_D was ~100 nM, and at 30 mM MgATP, ~500 nM. In contrast, in studies with 30 mM ATP without Mg^{2+} (data not shown), 30 mM Mg^{2+} without ATP (data not shown), or 10 mM MgAMP-PNP (Figure 7B), the apparent affinity of ring 2 for β-tubulin was not altered. These control studies do not support the possibility that the decreased affinities observed at high MgATP concentrations reflect salt effects.

The inset of Figure 7C shows a plot of K_D versus low concentrations of MgATP (where ring 2 is essentially free of MgATP). The apparent K_D increased from ~3 nM in the absence of nucleotide to ~26 nM at 0.5 mM MgATP (Table 1). This is attributed, as above (Figure 7A), to an inter-ring effect of the nucleotide in ring 1 on the affinity of ring 2 for β-tubulin. This increase provided an upper bound estimate of $\leq$250 μM for $K_{D,Nuc1}$, consistent with the MgATP dissociation constant value of 40 μM obtained by Melki et al. (*14*). The apparent K_D remained constant from 0.5 to 1 mM MgATP, and then *decreased* with MgATP concentrations of up to 4 mM. We tentatively attribute this decrease in K_D to a weakening of inter-ring communication followed by a recovery in the binding affinity of ring 2 for β-tubulin to values similar to the nucleotide-free case. A sharp, cooperative-like transition in the K_D values occurred between 4 and 6 mM MgATP where all or most of the subunits in ring 2 apparently took up MgATP. The estimated transition point, ~4.5−5.0 mM, provided us with an estimate for the apparent MgATP dissociation constant for ring 2 ($K_{D,Nuc2}$). The gradual decrease in K_D observed before the transition is consistent with a modified Koshland, Nemathy, and Filmer (KNF) model for cooperativity, where MgATP binding is sequential and indicative of a functional hierarchy in the subunits (*33*). Saturation of ring 2 with nucleotide after this transition is expected to give rise to a linear increase in the apparent K_D with increasing MgATP concentrations. Figure 7C shows plots of the apparent K_D versus MgATP concentration for two independent studies at high MgATP concentrations fitted to eq 2 (Experimental Procedures). Equation 2 predicts that as ring 2 saturates with MgATP, the apparent K_D for β-tubulin should increase linearly with MgATP concentration at an extent inversely proportional to $K_{D,Nuc2}$. The average value obtained for $K_{D,Nuc2}$ (3 mM) is ~100-fold greater than $K_{D,Nuc1}$. Our data therefore suggest that MgATP binding in ring 1 destabilizes MgATP binding to ring 2 by ~3 kcal/mol. The data thus supports inter-ring communication in CCT. As significant levels of intact CCT are apparently retained in vitro in the presence of moderate to high MgATP concentrations (Figure 7D), the study supports the notion that CCT can function as a two-stroke engine similar to GroEL. Further studies with saturating amounts of polypeptide will be required to confirm this hypothesis.

MgATP and MgAMP-PNP produce similar asymmetric structures when bound to ring 1 of CCT (*32*). The finding that MgAMP-PNP could not substitute for MgATP (Figure 7B) suggests that MgATP hydrolysis in ring 1 is required for weakening of inter-ring communication, thereby permitting MgATP binding to ring 2. In many MgATPases, AlF_4^- can replace transitorily bound phosphate produced by hydrolysis of ATP to generate a stable transition-state analogue (*47*, *48*). We thought it should be possible to exploit this

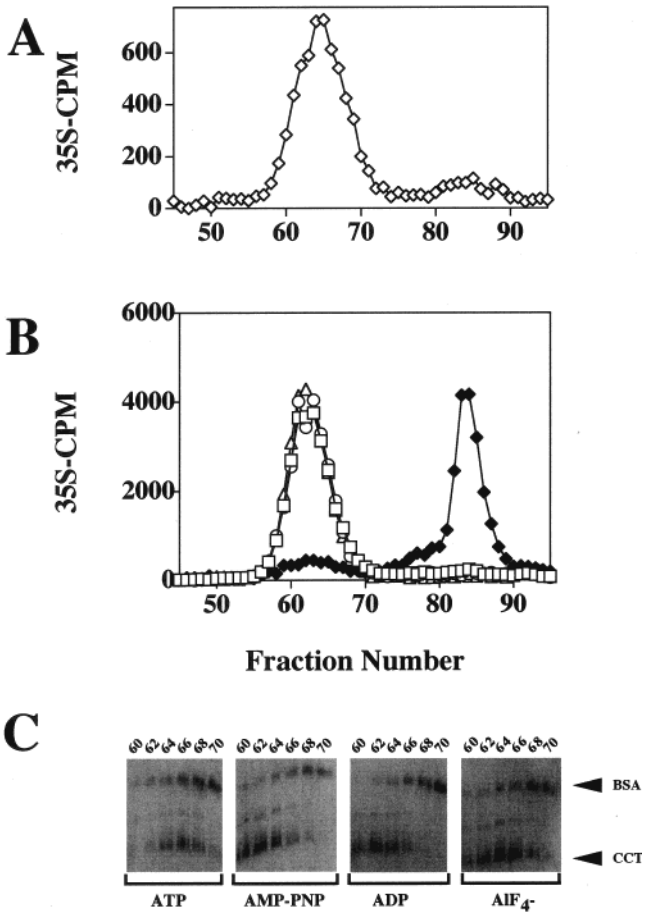

FIGURE 8: AlF_4^- stabilizes a low-affinity form of CCT in the presence of MgATP but not MgADP or MgAMP-PNP. (A) AlF_4^- study (100 μM). Purified CCT was diluted to 200 nM in folding buffer that contained 100 μM ATP, 100 μM $Al(NO_3)_3$, and 5 mM NaF and was incubated for 90 min. [^{35}S]-β-Tubulin was diluted 100-fold out of urea into CCT and incubated for 10 min. Samples were chromatographed on a Superose 6 column to assess binding affinities. The Mg^{2+} concentration was 2 mM. (B) AlF_4^- study (1 mM). Purified CCT was diluted to 200 nM in folding buffer supplemented with 1 mM $Al(NO_3)_3$ and 10 mM NaF (□) or, in addition, with 1 mM ATP (◆), ADP (△), or AMP−PNP (○) and incubated for 90 min. Samples were processed as described for panel A. (C) β-tub-CCT fractions 60−70 from the 1 mM studies were subjected to SDS−PAGE and silver staining.

stability to achieve nucleotide occupancy of ring 2 at much lower MgATP concentrations than that of Figure 7. CCT was incubated with 100 μM MgATP, 100 μM $Al(NO_3)_3$, and 5 mM NaF (*14*) and the binding affinity for β-tubulin assessed. The chaperonin retained a relatively high affinity for β-tubulin (apparent $K_D \sim 20$ nM, Figure 8A). However, when the concentrations were increased to 1 mM MgATP, 1 mM $Al(NO_3)_3$, and 10 mM NaF, a much lower apparent affinity was observed (apparent $K_D > 1$ μM, Figure 8B). ATP appeared to be limiting in the 100 μM study because increasing the concentrations of $Al(NO_3)_3$ and NaF was not sufficient to generate the low-affinity form (data not shown). The low-affinity state could not be obtained with MgADP−AlF_4^- or MgAMP-PNP−AlF_4^-, indicating that ATP hydrolysis was required (Figure 8B). Column fractions analyzed by SDS−PAGE and silver staining showed similar intensities and elution positions of CCT subunits for the ATP−AlF_4^-, ADP−AlF_4^-, AMP-PNP−AlF_4^-, and AlF_4^- samples, indicating that the chaperonin was intact (Figure 8C).

DISCUSSION

Comparison of K_D Values with Previous Studies. The apparent K_D values for β-tubulin and actin binding to CCT (Table 1) are similar to K_D values commonly observed for tight binding substrates of GroEL. However, they are smaller by 2 orders of magnitude than those reported previously (*14*). With the exception of 100 mM KCl present in our folding buffer, the folding buffers are essentially identical in the two studies. When we repeated the K_D measurements for wild-type β-tubulin in the previously used buffer (*14*), values similar to those reported in Tables 1 and 2 again were obtained. We therefore attribute the discrepancy in the apparent K_D values to differences in experimental design. In the study presented here, the apparent K_D values that were obtained were ascribed to polypeptide binding at ring 1 (Results). The CCT concentration was varied, while a fixed limiting concentration of substrate was used (typically 1.5 nM, which is lower than the experimentally determined K_D). In contrast, Melki et al. *did a saturation study*, varying substrate over a range of concentrations that were in considerable excess of their K_Ds (from 350 nM to 25 μM in the case of β-tubulin) while holding the CCT concentration fixed at 500 nM. They concluded that at saturation two β-tubulins bound CCT with apparently identical affinities (K_Ds $\sim$ 1 μM). One β-tubulin was assigned to each ring, and the binding of the two β-tubulins to the two rings was assumed to occur simultaneously (their Figure 8). The high K_D value they deduced likely reflects binding of the second β-tubulin to ring 2 since our results indicate that ring 1 would have already been saturated with β-tubulin polypeptide at the very start of their concentration study [their first data point at 350 nM in fact shows 6 pmol of β-tubulin bound per 10 pmol of CCT (60% saturation)]. For the previous investigators to have studied binding to ring 1, they would have had to reduce their CCT and β-tubulin concentrations by *more than 2 orders of magnitude*.

CCT Substrate Selectivity. The class II chaperonin CCT facilitates the folding of actin, tubulin, G_α transducin, cyclin E, and probably myosin II (*49*) in vitro and in vivo. Thus far, in vivo studies have failed to clearly identify any other substrate proteins; however, recent evidence suggests that perhaps as much as 10% of newly synthesized proteins in mammalian cells may transit through CCT (*50*). When presented from denaturant, most proteins do not bind to CCT with high affinity (G. W. Farr, unpublished observations). Nevertheless, Melki et al. have proposed that a significant number of denatured proteins bind with high affinity to CCT in vitro (*14*). In contrast, the class I chaperonin GroEL has been shown to facilitate the folding of many proteins in vitro and is thought to interact with many more proteins in vivo (*51*−*53*). Several studies have recently attempted to explore the apparent selectivity of CCT by using mutagenesis to alter the primary structures of actin or tubulin (*2*, *3*). These investigations were limited by the fact that (i) controls were not introduced to test the possibility that a change in the primary structure significantly altered the conformation of the substrate protein presented to CCT and (ii) the assays failed to quantitate sufficiently the binding affinities.

In the current study, we introduced ftsZ/β-tubulin chimeras as potential controls and implemented a quantitative approach to determine the contribution of select regions of β-tubulin

to binding. Our results indicate that the concept of a high-affinity interactive core which is restricted to a defined region in the substrate protein and accounts for CCT's substrate selectivity is illusory (see below). However, certain sites (hot spots) may interact modestly with CCT. We identified one such site at residues 259−272 by alanine scanning mutagenesis. Nevertheless, our use of other mutants as probes to identify additional hot spots met with little success. This failure may reflect the possibility that β-tubulin fragments and scanning alanine mutants perturbed the conformation of the folding intermediate and in so doing have smoothed out the contribution of other hot spots. However, it is unlikely that such perturbations masked large ΔG contributions. For instance, when the N-terminal fragments and their corresponding N-terminal chimeras are compared, there is little difference in the binding free energies ($\leq$1 kcal/mol, Table 2). We are thus confronted with an inability to rationalize β-tubulin's high apparent affinity for CCT in terms of interactions with select β-tubulin regions.

Our finding of weak binding sites in β-tubulin that lead to high-affinity association with CCT suggests, as one possibility, active involvement of CCT. This anomaly was also noted in the recent study of actin binding to CCT, where positive cooperative interactions between CCT and the weak binding sites in actin were hypothesized as a mechanism for strengthening binding (*2*, *3*). Positive cooperative interactions may contribute to β-tubulin binding, although we have no evidence for this at present. In contrast, negative inter-ring cooperativity may be important for β-tubulin binding as suggested by the large discrepancy in the binding affinities of β-tubulin for the two rings of CCT (our study versus Melki et al., Results). If so, the 2 order of magnitude discrepancy in K_D values suggests a ~3 kcal/mol increase in the binding free energy for ring 2 relative to that for ring 1. This increase is similar to that estimated earlier for MgATP binding to ring 2 relative to binding to ring 1 (Figure 7C).

Role of the Chaperonin in Substrate Binding. While comparing the affinities of the N- and C-terminal chimeras, we were struck by a consistent excess of free energy in each matched pair (Table 3). We had anticipated that the sum of the free energies for the binding of a matched pair would be roughly equal to the free energy observed for intact wild-type β-tubulin. Instead, this sum shows a *consistent* excess of −7 kcal/mol of free energy when compared with wild-type β-tubulin (Table 3, $\Delta G_{N+C} - \Delta G_{WT}$ varied from −6.9 to −7.1). This discrepancy may reflect folding differences between the wild type and the chimeras. Alternatively, if the ftsZ portions of the chimeras make an insignificant (<10%) contribution and the intrinsic contributions from the β-tubulin portions of the chimeras are more or less equivalent to the same regions in wild-type β-tubulin, this additional free energy suggests contributions from sources other than the bound polypeptide. One possibility is that the chaperonin itself, perhaps by a conformational change, stabilizes the binary complex by providing additional negative binding free energy. If true, then this stabilizing energy should appear twice in the sum of the ΔGs of the matched pair, a consequence of two separate binding measurements, compared with just one measurement for wild-type β-tubulin, and should be evident as an additional ΔG (estimated here to be −7 kcal/mol) when the binding free energies are compared. This presumptive contribution of ca. −7 kcal/mol from CCT is uncorrected for differences in intramolecular folding of tubulin and chimeras and is an upper bound estimate. It is possible that in the chimeras, the domains may pack against each other differently than in wild-type β-tubulin. This could expose additional β-tubulin sites for interaction with CCT and contribute to the excess ΔG. Whether these and other intramolecular folding differences would be large enough to account for the −7 kcal/mol excess free energy, an amount that is *~60% of the total binding free energy of wild-type β-tubulin*, is unclear to us in view of the considerable structural similarity of native ftsZ and β-tubulin (*39*, *44*) (Figure 5A). Furthermore, the fact that all three chimera pairs give the identical excess free energy within a few percent (Table 3) seems not to support this possibility. In contrast, the hypothesis that a conformation change in CCT occurs concomitant with substrate binding readily rationalizes this constancy.

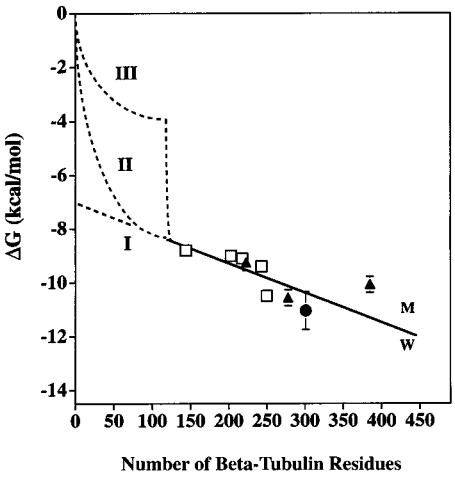

FIGURE 9: Apparent ΔG vs the number of β-tubulin residues (residue length). Apparent ΔG values are shown for the N-terminal fragments and N-terminal chimeras (□), the wild type (**W**), Mut. 1 (**M**), internal deletions Δ85−144, Δ86−251, and Δ85−306 (▲), and N-terminal deletion mutant Δ2−145 (●). The solid line, where apparent ΔG(kcal/mol) = −7.5−0.009 × residue length, is a least-squares fit to the data. Values for the internal deletions and Δ2−145 are based on single-CCT concentration studies. Three different scenarios for ΔG at short residue lengths (<100) are also sketched in this figure (dashed lines I−III). See the text for details.

This additional free energy was also encountered in a more complete analysis of our binding data. Figure 9 shows apparent ΔG values for the wild type, N-terminal fragments, and N-terminal chimeras (primary data taken from Tables 1 and 2) together with three internal deletion fragments Δ85−144, Δ86−251, and Δ85−306, and an N-terminal deletion mutant Δ2−145 from Dobrzynski et al., plotted against the number of β-tubulin residues present in the respective polypeptides ("residue length"). ΔG values fit a least-squares line [slope = −9 cal mol^{-1} (β-tubulin residue)$^{-1}$]. The data represent a range of more than 2 orders of magnitude in K_D values. We were unable to detect binding of the fragment 1−85 (the smallest fragment we examined) by our technique (<1% bound at 200 nM CCT; K_D > 10 μM) (*3*). We conservatively estimated that the K_D for deletion mutant Δ85−144 was ~50 nM. Compared with that of the wild type, this represents an increase in free energy from −11.8 to −10.2 kcal/mol (Figure 9, ▲ at residue length 385 vs **W** at residue length 445). The difference of 1.6 kcal/mol is greater than what would be expected if residues 85−144 made an

"average" contribution of ca. −9 cal mol^{-1} (β-tubulin residue)$^{-1}$ to binding, a result which suggests that this region contains a hot spot[2] (the significance of this "average" contribution is discussed below). The apparent linear dependence of Δ*G* on residue length (Figure 9) does not support the existence of a major region of β-tubulin, such as an interactive core (*3*), which gives rise to CCT specific binding. Furthermore, the finding that the wild-type value falls on or close to this least-squares line does not support the positive cooperativity model of Rommelaere et al. (*2*).[3] More importantly, the linear plot implies that β-tubulin interactions with CCT are to a good approximation additive over a wide range of fragment and domain sizes and supports the notion that the excess free energy derived in Table 3 arises from factors other than differences in folding. Further studies will be required to confirm these findings. It should be noted that we do not interpret the linear plot (solid line, Figure 9) as evidence that the bound forms are unfolded on the interior surface of CCT and that interactions with the chaperonin are equal along the entire length of the protein with individual residues generally contributing ca. −9 cal/mol to Δ*G*. Rather, we believe these forms are quasi-native (wild type) (ref *3* and Figure 6B) or quasi-native and/or molten globule (mutants) and have multiple weak binding sites (together with several moderate hot spots) which are distributed along the β-tubulin sequence and which give rise to the apparent linear dependence of Δ*G* on residue length. The number and location of these sites are largely unknown.

We suggest the least-squares slope [−9 cal mol^{-1} (β-tubulin residue)$^{-1}$] (Figure 9) provides a *global* average of the interaction of CCT with the β-tubulin residues, *valid for polypeptides that contain >100−140 β-tubulin residues* (see below). As defined, this global average includes *all* β-tubulin residues in the folding intermediate, both buried and exposed (Experimental Procedures). Surprisingly, this measure of interaction is apparently constant and to a good approximation independent of polypeptide size for fragments with more than ∼140 residues. This can be understood if the polypeptides are largely unfolded on the interior surface of CCT. We do not believe this to be the case and favor a dynamic model of interaction to explain the result. We suggest that the bound polypeptides interact dynamically with CCT at multiple weak binding sites with transient exposure of "buried residues" to CCT being a frequent occurrence. This concept is developed further below. Other explanations are possible. For example, an ensemble of bound forms that interact statically with CCT might also give rise to an apparent linear dependence of Δ*G* on β-tubulin length.

A globally averaged contribution of ca. −10 to −11 cal/mol per β-tubulin residue similar to that derived from Figure 9 was also obtained for the wild type and chimeras by an *entirely different* approach (above) when binding free energies were corrected for a putative conformation change in CCT (Table 3, column 4 and footnote d). In contrast, the *uncorrected* globally averaged contribution ranged from ca. −27 cal mol^{-1} (β-tubulin residue)$^{-1}$ for the wild type (−11.8 kcal/mol per 445 residues) to ca. −45 cal mol^{-1} (β-tubulin residue)$^{-1}$ for the chimeras (values in column 1 of Table 3 divided by the number of β-tubulin residues). While we cannot definitively say at present which version is correct, we find it satisfying that the globally averaged contributions are apparently similar when corrected for the putative conformation change in CCT. This suggests that intramolecular folding may not be very different in the wild type and chimeras. In our analysis (Table 3), we assumed as a working hypothesis that β-tubulin fragments and/or domains contribute additively to the energy of binding. This hypothesis is supported by the Figure 9 results and implies that each domain or fragment interacts independently with CCT, without major steric interference, in a manner similar to that of the corresponding region in the wild type. This cannot be strictly correct. The assumption of additivity, however, may pose less of a problem than one might initially think. We observed, for example, that the apparent K_Ds of the N-terminal chimera differed by no more than a factor of 2−5 from those of the N-terminal fragments. This translates to a relatively modest difference of ∼0.5−1 kcal/mol in their binding free energies *despite* the fact that the fragment set lacks a C-terminal domain, whereas the chimera set nominally has C-terminal domains that are structurally similar to those of β-tubulin and ftsZ (Figure 4A). Whether these C-terminal domains pack against the N-terminal domains in a similar manner as in the wild-type folding intermediates is presently unknown.

In Figure 9, we sketched three hypothetical scenarios for β-tubulin residue lengths of <100: (I) β-tubulin residues continue to contribute ca. −9 cal mol^{-1} residue^{-1} and the least-squares line intercepts the *Y*-axis at ca. −7.5 kcal/mol (zero residue length); (II) Δ*G* decreases with decreasing β-tubulin residue length and extrapolates to 0 kcal/mol at zero residue length (i.e., molecular interactions between β-tubulin and CCT are entirely responsible for the free energy of binding); and (III) Δ*G* behavior is intermediate between that in scenarios I and II (i.e., we hypothesize a discontinuity in Δ*G*).

Scenario I yields an intercept value that is in excellent agreement with the additional free energy observed with the matched chimeras and is consistent with the notion of a stabilizing conformation change in CCT. However, Scenario I seems simplistic. Bearing in mind the surface to volume changes expected with polypeptide size, the potential for a residue to interact with CCT should *increase* as polypeptide size decreases as more residues would be at the surface and fewer would be buried in the interior. The slope of the Δ*G* plot would therefore be expected to increase and become steeper as residue length decreased toward 0, with the intercept on the *Y*-axis possibly occurring at or near Δ*G* = 0. Scenario II shows this behavior.

Scenario II assumes that short polypeptides are well behaved and ignores the possibility that these polypeptides interact dynamically with CCT which was implicit in scenario I. Scenario III (Figure 9) makes the additional

[2] Native β-tubulin contains two protease-sensitive regions, PS1 and PS2 (residues 120−160 and 260−290, respectively) (*1*) (Figure 1A). Hot spot 259−272 falls in PS2; this second hot spot between residues 85 and 144 overlaps PS1. Rommelaere et al. showed that actin contains three major recognition sites for CCT, i.e., residues 125−179, 244−285 (contains the hydrophobic plug), and 340−375 (*2*). One of the sites is weakly homologous to HR2 (*2*; see also ref *3*) (Figure 1A) and another to protease-sensitive region PS1 (*4*) (Experimental Procedures).

[3] Our data do not exclude the possibility that hot spots contribute cooperatively to Δ*G*. However, in contrast to Rommelaere et al., we believe that if such interactions are present they are secondary to other factors, e.g., a stabilizing conformation change in CCT, which we propose accounts for the major portion of the binding free energy (see the text).

assumption (discussed below) that a certain critical size or volume of polypeptide induces a conformation change in CCT which stabilizes binding (see below). In Figure 9, ΔG is arbitrarily shown as decreasing at a modest rate from 0 kcal/mol at 0 residues to ca. −2 to −4 kcal/mol at 70−120 residues, whereupon a rapid decrease to ca. −8 to −9 kcal/mol indicative of the conformation change in CCT occurs, followed by the much slower rate of decrease described earlier for the least-squares line shown in Figure 9 (∼9 cal mol^{-1} $residue^{-1}$). In this scenario, linear extrapolation of the least-squares line toward the *Y*-axis (done inappropriately in scenario I) extends ΔG into a virtual region that ignores the discontinuity; the intercept value obtained, −7.5 kcal/mol, provides an upper bound estimate of the contribution of CCT to ΔG valid only *for residue lengths of >70−100*, i.e., for polypeptides greater than a critical size. This estimate is similar to that derived in Table 3. Scenario III is arbitrarily depicted in Figure 9. We have no data that indicate where the discontinuity occurs, nor do we know its magnitude or whether it actually occurs. The quantitative aspects, as well as the validity of scenarios II and III, need to be addressed in a separate study (the studies would be technically difficult but should be feasible).

We think the alternative explanation which ascribes the excess ΔG in Table 3 to differences in folding (above) is inadequate. It ignores what we believe to be compelling arguments for a stabilizing contribution from CCT. Two independent approaches, one based on an analysis of the paired chimeras and a second on a more complete data set, gave similar upper bound estimates for the contribution of this conformation change to ΔG and similar estimates of the global average contribution of the β-tubulin residues to the binding free energies. We suggest that the excess ΔG in Table 3 very likely reflects two contributions: one from a conformation change in CCT which stabilizes the binding and a smaller contribution from folding differences between the wild type and chimeras. If our conjecture is correct, the apparent stabilization energy could be ∼4−7 kcal/mol, allowing for experimental uncertainties. This corresponds to a modest ∼0.5−0.9 kcal/mol contribution per CCT subunit if the conformation change occurs cooperatively and is limited to ring 1 (all eight subunits assumed to behave equivalently). There are other explanations for the excess ΔG. Although our data suggest otherwise, we cannot exclude the possibility that ftsZ residues contributed significantly to the excess ΔG. Furthermore, if CCT dissociated at high dilutions ([CCT] < 4 nM), we may have underestimated its affinity for wild-type β-tubulin. If we assume an apparent K_D of ∼50 pM for the wild type ($\Delta G_{WT} = -14$ kcal/mol), we obtain an upper bound estimate of ca. −4 to −5 kcal/mol for CCT's contribution. To contravene our hypothesis, the K_D for the wild type would need to be in the high femtomolar range, ∼3−4 orders of magnitude lower than the value we report (Table 1). This seems unreasonable. The affinity of ring 1 for β-tubulin would be almost 5−6 orders of magnitude greater than that of ring 2 (see above). Apparent hot spot HR2 would now contribute >5 kcal/mol to binding (Mut. 1 vs the wild type). This translates to an apparent K_D of <100 uM for this region alone. Fluorescence quenching studies with MCA residues 251−288, a methylcoumarin derivative of a synthetic peptide that encompassed the HR2 region (QCB Biochemicals; studies to ∼40 μM peptide), failed to detect any interaction with CCT (R. Melki and H. Sternlicht, unpublished studies).

The structural changes in CCT that we propose are induced by β-tubulin binding are presently unclear. One possibility is that insertion of polypeptide into ring 1 expands CCT as occurs with GroEL and GroES. Like GroEL, CCT has a hinged region that ought to allow this expansion. Accompanying this "mechanical" expansion may be small local changes in CCT that bring positive charges closer to negative charges and/or hydrophobic residues closer to other hydrophobic residues, etc., which collectively contribute −4 to −7 kcal/mol to ΔG. Alternatively or in addition, CCT may *partially encapsulate* the bound polypeptide, which would help stabilize binding. This possibility is supported by EM studies, which suggest that CCT can encapsulate substrate released into its channel following MgATP binding or hydrolysis (*23*). On the basis of the latter studies, the following scenario could apply: (i) β-tubulin binds to the apical domains and inserts into CCT; (ii) insertion deforms CCT, causing a rotation of its apical domains and a partial sequestration of the polypeptide binding residues, which reduces the affinity for β-tubulin; and (iii) simultaneously, helical protrusions present at the apical domain tips of CCT are exposed (*23*) and partially encapsulate β-tubulin which reduces its off-rate. In the presence of MgATP, larger rotations of the apical domains are induced. The helical protrusions now seal the central cavity, encapsulating the β-tubulin released into the cavity. This scenario supports the hypothesis that chaperonin and co-chaperonin functions are subsumed within CCT (*21, 22*).

Deformation Binding and Substrate Selectivity. We suggest that ΔG is a composite of two terms, ΔG_{Stab} and ΔG_{Int}, where ΔG_{Stab} denotes the contribution from CCT and ΔG_{Int} ($=RT \ln K_{D,Int}$) denotes the residual (intrinsic) binding free energy of the polypeptide. For a ΔG_{Stab} of −6 kcal/mol, ΔG_{Int} would be −6 kcal/mol for the wild type which translates to an apparent $K_{D,Int}$ of ∼40 μM. Much larger $K_{D,Int}$ values are obtained for the fragments. Paradoxically, ΔG_{Int} on its own appears to be generally *insufficient* to support polypeptide binding. We propose that in eukaryotes an **R** form of CCT separated from *a more stable* **T** form by a high activation barrier predominates in the absence of substrate. The **R** form has relatively high intrinsic affinity for substrates. [This differs from the MWC model (*54*) where a low-affinity form would predominate in the absence of substrate.] Binding of substrate (**S**) lowers the activation barrier and induces the **T** form, which has a reduced intrinsic affinity for substrate (as "measured" by $K_{D,Int}$). The bound complex **T·S** has a lower apparent free energy than **R·S** and is the form detected in this study. Upon dissociation of **S**, we hypothesize that **T** reverts back to **R**. Unlike the MWC model which requires that **T** and **R** maintain the 8-fold "symmetry" of the complex, **T** and **R** in our model need not maintain this symmetry. The binding reaction can be represented as Scheme 1, shown below. While it is useful to discuss $K_{D,Int}$ as if it has a physical reality and relates to an equilibrium between **S** and **T**, free **T** is only very slowly obtained from **R** and bound **T** is obtained mainly as a consequence of the binding of **S** to **R**. Scheme 1 is based on the nucleotide-free case. It may also apply to the MgADP case. This scheme is different from an "induced fit", where substrate affinity for induced **T** markedly increases as the binding site is structurally altered to

Scheme 1

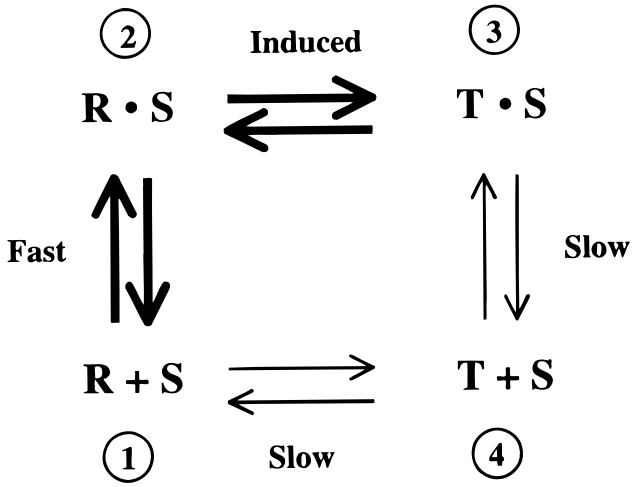

accommodate the substrate. In Scheme 1, the intrinsic affinity of the substrate for induced **T** is at most the same as that for **R**. More likely, it is reduced relative to that for **R**.

We speculate that there are two major classes of non-native polypeptides that bind CCT. One class binds to **R** but does not induce a transition to **T**. Polypeptides in this class are presumed to transit through the chaperonin, perhaps in some cases binding with high affinity to **R**, but their folding is not dependent on CCT. The second class binds to **R** and induces a transition to **T**. This class includes substrates such as tubulin and actin, which require interaction with CCT for their productive folding. The basis for the transition is not known but may require an interaction of CCT with some recognition feature(s) in the conformation or sequence of the polypeptides[2] and/or perhaps "triggering" interactions with one or more specific subunits in CCT (*33*). An alternative possibility which we find attractive is that the transition is not limited to a select number of substrates but that many non-native polypeptides (M_r < 100 kDa) with a sufficiently large volume can induce this transition. However, only a select number are retained by CCT (i.e., have a sufficiently low $K_{D,Int}$). Although we do not believe that synergistic and/or cooperative interaction between hot spots as proposed previously is responsible for the high affinity of binding of tubulin and actin to CCT (*2*), such interactions could be important for $K_{D,Int}$ and for CCT selectivity. The finding of a second potential hot spot in β-tubulin (▲ at residue length 385, Figure 9) that, like the earlier hot spot HR2, is homologous to a putative hot spot in actin lends credence to the notion that conserved regions in tubulin and actin play a critical role in CCT function.[2]

In Scheme 1, **T·S** is shown as potentially dissociating into **T** and **S**. In time, **T** would be expected to accumulate and eventually disrupt function. **R** is also shown as "metastable" with the potential to convert to **T** in the absence of substrate. However, we have seen no evidence for this. [CCT incubated with or without ATP at 30 °C for more than 24 h is stable and binds substrates with affinities similar to those reported in our binding studies (unpublished observations).] In vivo, CCT undergoes disassembly and reassembly cycles dependent on ATP as well as accessory proteins whose function is not understood (*46*). These cycles are thought to be involved in CCT biosynthesis (*38*) and may be an integral part of the protein folding mechanism of CCT (*5*, *46*). An intriguing possibility is that cycling is needed for disassembly of accumulated **T** and reassembly of the products into fresh **R**.[4]

Dynamic Unfolding or Refolding on CCT. If polypeptide binding is linked to a conformation change in CCT, high-affinity binding to the chaperonin can be achieved with a low "intrinsic" affinity for polypeptide. If β-tubulin hot spots could be painted with different colors and if we could look down the central channel, we would expect to see a kaleidoscope of colors, flickering and changing in an apparently random manner over time, as these sites bind to and are released from various contact points on the chaperonin. Taking snapshots should reveal an ensemble of colored positions that reflect different molecular configurations of the polypeptide. ATP hydrolysis induces release of bound polypeptide into the central channel to complete folding. In this dynamic model, catalytic efficiency (as measured by the number of productive folding intermediates per folding cycle) depends on the fraction of configurations in the ensemble that are competent to fold productively once released into the channel. It is possible in the case of β-tubulin that this process proceeds in stages that resemble maturation such that early productive intermediates are transformed into late productive intermediates. Alternative dynamic models based on rotational diffusion of substrate within the channel or that permit some cooperative interactions with CCT are possible. Also, hot spots need not play as major a role. We have been puzzled for some time by proteolytic results, which show complex degradation of CCT-bound β-tubulin. This unusual result may reflect ready accessibility of bound substrate to protease perhaps because of fenestrations in CCT [fenestrations are observed in the thermosome (*21*) and GroEL (*31*)]. However, it could also be indicative of dynamic folding. According to the dynamic model, a protease would see an ensemble of forms with different channel and/or fenestrated aspects and could generate a complex fragmentation pattern. Complex fragmentation patterns have also been seen with GroEL-bound substrate (*55*, *56*) and may originate from similar dynamic interactions.

We suggest that dynamic interactions between CCT and substrate enhance catalytic efficiency and the productive folding of substrate once released into the central cavity. It is conceivable that dynamic interactions also permit folding on the interior surface of CCT prior to release into the central cavity. Such folding could facilitate changes in the tertiary interactions of early intermediates and contribute to substrate maturation. Coyle et al. (*57*) recently reported that GroEL accelerates the refolding of hen lysozyme in the absence of MgATP. This facilitation occurs on the interior surface of GroEL. Shtilerman et al. also recently reported that ATP binding to GroEL unfolds a kinetically trapped intermediate of RuBisCo. This unfolding is hypothesized to occur through

[4] The conformational cycle and protein binding properties of the archaeosome, a class II chaperonin with heat-shock function from *Sulfolobus shibatae* (*5*), are explained by Scheme 1 if the two major forms of the archaeosome, i.e., the closed and open forms, correspond to **T** forms in the absence or presence of ATP, respectively. We suggest that a minor form in the **R** state, not detected by the investigators, initially binds unfolded protein (derived from a protein pool complexed with free archaeosome subunits as described by the investigators). This form presumably converts to the **T** form during the induction step **(R·S → T·S)** and is regenerated in subsequent disassembly and assembly cycles of the archaeosome.

ATP-induced movements of the apical domains of GroEL (*58*). CCT may also use a repertoire of mechanisms to facilitate substrate folding.

Binding in the Presence of Nucleotide. Indirect binding studies with β-tubulin suggest a nested cooperativity in MgATP binding to CCT (Figures 6 and 7), as is observed for GroEL. Hydrolysis in ring 1 of GroEL or GroES permits ring 2 to be occupied with nucleotide (*24*, *28*). A similar requirement was observed here with CCT. Binding to ring 2 occurred at high MgATP concentrations (>4 mM) under our substrate limiting conditions. We do not know the effect of polypeptide on this binding. Our study described above carried out in the absence of nucleotide suggests a much more active role for polypeptide in chaperonin function than previously realized. One possibility is that polypeptide release into channel 1 by nucleotide binding or hydrolysis induces a conformation change in ring 1 (different from the one induced by bound polypeptide in the absence of nucleotide) which *weakens* inter-ring communication, permitting MgATP binding to ring 2 at lower concentrations. This contrasts with our earlier proposal that β-tubulin bound to ring 1 (no nucleotide) *strengthens* inter-ring communication, i.e., causes a reduction in the affinity of ring 2 for β-tubulin (our study vs Melki et al.). Nucleotide binding studies carried out under saturating conditions of β-tubulin are required to test this hypothesis. We observed a profound effect of AlF_4^- on β-tubulin binding in the presence of MgATP (Figure 8B). In its absence, comparable effects would only be seen with MgATP concentrations of $>30-50$ mM. It is intriguing to speculate that in the presence of polypeptide the $ADP-PO_4^{3-}$ transition state complex may be relatively long-lived and, either on its own or together with polypeptide, causes the conformation change that efficiently weakens inter-ring communication in CCT.

Conclusions. We have proposed a new and *provocative* model for CCT function. β-Tubulin−CCT interactions involve multiple relatively weak binding sites in ill-defined quasi-native folding intermediates which makes their study difficult. While our data that support the model are internally consistent, a major unresolved question relates to the apparent additivity of the β-tubulin residue interactions with CCT manifested by the apparent linear dependence of ΔG on residue length. We suspect these features reflect in part the dynamic nature of the interactions of the β-tubulin polypeptides with CCT. A definitive test of our model will likely require transient kinetic analysis in identifying the CCT intermediate. It should be possible to introduce fluorophores into the polypeptide binding regions of CCT directly or by in vitro synthesis followed by subunit exchange (*38*). Recent kinetic analysis of the nucleotide-induced allosteric transitions of GroEL revealed a rich repertoire of structural rearrangements preceding hydrolysis which presently are not well-understood (*59*). It is likely that a rich repertoire of structural rearrangements will also be seen upon binding of substrate to GroEL and CCT.

NOTE ADDED IN PROOF

Llorca et al. recently reported a three-dimensional reconstruction of an α-actin−CCT complex obtained by cryo-electron microscopy in the absence of nucleotide (*60*). While potential differences exist between the two studies, the EM study is consistent with our major conclusions. For example, the authors report the binding of a *single* actin molecule to CCT under their experimental conditions ($\leq$10-fold excess of substrate to CCT). They also report that α-actin and β-actin.sub4, a chimeric protein containing subdomain 4 of β-actin fused to the C-terminus of the Ha-Ras protein, induce a *concerted conformation change* in CCT upon binding (Ha-Ras serves a similar control function in their study as ftsZ does in our study). Finally, they observed that α-actin bound either to the CCTδ and CCTϵ subunits or to the CCTδ and CCTβ subunits, consistent with our proposal of an *ensemble of folding configurations* for CCT substrates in the central cavity.

ACKNOWLEDGMENT

We thank Piet de Boer for his gift of a T7-based ftsZ expression vector and Mike Maguire for urging the construction of the β-tubulin/ftsZ chimera proteins (also for helpful discussions). We also thank Eva Nogales and Ken Downing (for the ribbon diagrams of β-tubulin and ftsZ shown in Figure 4A), Tony Berdes and John Mieyal for helpful discussions, and Avron Horovitz and F. Ulrich Hartl for critical comments on the manuscript. We especially thank Ron Melki for his assistance with the fluorescence quenching experiments.

REFERENCES

1. de la Vina, S., Andreu, D., Medrano, F. J., Nieto, J. M., and Andreu, J. M. (1988) *Biochemistry 27*, 5352−5365.
2. Rommelaere, H., De Neve, M., Melki, R., Vandekerckhove, J., and Ampe, C. (1999) *Biochemistry 38*, 3246−3257.
3. Dobrzynski, J. K., Sternlicht, M. L., Farr, G. W., and Sternlicht, H. (1996) *Biochemistry 35*, 15870−15882.
4. Needleman, S. B., and Wunsch, C. D. (1970) *J. Mol. Biol. 48*, 443−453.
5. Quaite-Randall, E., Trent, J. D., Josephs, R., and Joachimiak, A. (1995) *J. Biol. Chem. 270*, 28818−28823.
6. Gao, Y., Thomas, J. O., Chow, R. L., Lee, G. H., and Cowan, N. J. (1992) *Cell 69*, 1043−1050.
7. Yaffe, M. B., Farr, G. W., Miklos, D., Horwich, A. L., Sternlicht, M. L., and Sternlicht, H. (1992) *Nature 358*, 245−248.
8. Farr, G. W., Scharl, E. C., Schumacher, R. J., Sondek, S., and Horwich, A. L. (1997) *Cell 89*, 927−937.
9. Won, K. A., Schumacher, R. J., Farr, G. W., Horwich, A. L., and Reed, S. I. (1998) *Mol. Cell. Biol. 18*, 7584−7589.
10. Eggers, D. K., Welch, W. J., and Hansen, W. J. (1997) *Mol. Biol. Cell 8*, 1559−1573.
11. Rommelaere, H., Van Troys, M., Gao, Y., Melki, R., Cowan, N. J., Vandekerckhove, J., and Ampe, C. (1993) *Proc. Natl. Acad. Sci. U.S.A. 90*, 11975−11979.
12. Kubota, H., Hynes, G., Carne, A., Ashworth, A., and Willison, K. (1994) *Curr. Biol. 4*, 89−99.
13. Liou, A. K. F., and Willison, K. R. (1997) *EMBO J. 16*, 4311−4316.
14. Melki, R., Batelier, G., Soulie, S., and Williams, R. C., Jr. (1997) *Biochemistry 36*, 5817−5826.
15. Marco, S., Carrascosa, J. L., and Valpuesta, J. M. (1994) *Biophys. J. 67*, 364−368.
16. Tian, G., Vainberg, I. E., Tap, W. D., Lewis, S. A., and Cowan, N. J. (1995) *J. Biol. Chem. 270*, 23910−23913.
17. Tian, G., Lewis, S. A., Feierbach, B., Stearns, T., Rommelaere, H., Ampe, C., and Cowan, N. J. (1997) *J. Cell Biol. 138*, 821−832.
18. Vainberg, I. E., Lewis, S. A., Rommelaere, H., Ampe, C., Vandekerckhove, J., Klein, H. L., and Cowan, N. J. (1998) *Cell 93*, 863−873.

19. Hansen, W. J., Cowan, N. J., and Welch, W. J. (1999) *J. Cell Biol. 145*, 265−277.
20. Siegers, K., Waldmann, T., Leroux, M. R., Grein, K., Shevchenko, A., Schiebel, E., and Hartl, F. U. (1999) *EMBO J. 18*, 75−84.
21. Ditzel, L., Lowe, J., Stock, D., Stetter, K.-O., Huber, H., Huber, R., and Steinbacher, S. (1998) *Cell 93*, 125−138.
22. Klumpp, M., Baumeister, W., and Essen, L.-O. (1997) *Cell 91*, 263−270.
23. Llorca, O., Smyth, M. G., Carrascosa, J. L., Willison, K. R., Radermacher, M., Steinbacher, S., and Valpuesta, J. M. (1999) *Nat. Struct. Biol. 6*, 639−642.
24. Xu, Z., and Sigler, P. B. (1998) *J. Struct. Biol. 124*, 129−141.
25. Rye, H. S., Roseman, A. M., Chen, S., Furtak, K., Fenton, W. A., Saibil, H. R., and Horwich, A. L. (1999) *Cell 97*, 325−338.
26. Lorimer, G. (1997) *Nature 388*, 720−723.
27. Hayer-Hartl, M. K., Ewalt, K. L., and Hartl, F. U. (1999) *Biol. Chem. Hoppe-Seyler 380*, 531−540.
28. Rye, H. S., Burston, S. G., Fenton, W. A., Beechem, J. M., Xu, Z., Sigler, P. B., and Horwich, A. L. (1997) *Nature 388*, 792−798.
29. Mayhew, M., Silva, A. d., Martin, J., Erdjument-Bromage, H., Tempst, P., and Hartl, F. (1996) *Nature 379*, 420−426.
30. Weissman, J., Rye, H., Fenton, W., Beecham, J., and Horwich, A. (1996) *Cell 84*, 481−490.
31. Braig, K., Otwinowski, Z., Hegde, R., Boisvert, D. C., Joachimiak, A., Horwich, A. L., and Sigler, P. B. (1994) *Nature 371*, 578−586.
32. Llorca, O., Smyth, M. G., Marco, S., Carrascosa, J. L., Willison, K. R., and Valpuesta, J. M. (1998) *J. Biol. Chem. 273*, 10091−10094.
33. Lin, P., and Sherman, F. (1997) *Proc. Natl. Acad. Sci. U.S.A. 94*, 10780−10785.
34. Melki, R., and Cowan, N. J. (1994) *Mol. Cell. Biol. 14*, 2895−2904.
35. Tian, G., Vainberg, I. E., Tap, W. D., Lewis, S. A., and Cowan, N. J. (1995) *Nature 375*, 250−253.
36. Vallejo, A. N., Pogulis, R. J., and Pease, L. R. (1995) in *PCR Primer: A laboratory manual* (Dieffenbach, C. W., and Dveksler, G. S., Eds.) pp 603−612, Cold Spring Harbor Laboratory Press, Plainview, NY.
37. Gao, Y., Vainberg, I. E., Chow, R. L., and Cowan, N. J. (1993) *Mol. Cell. Biol. 13*, 2478−2485.
38. Liou, A. K., McCormack, E. A., and Willison, K. R. (1998) *Biol. Chem. Hoppe-Seyler 379*, 311−319.
39. Nogales, E., Wolf, S. G., and Downing, K. H. (1998) *Nature 391*, 199−203.
40. Kyte, J., and Doolittle, R. F. (1982) *J. Mol. Biol. 157*, 105−132.
41. Nogales, E., Whittaker, M., Milligan, R. A., and Downing, K. H. (1999) *Cell 96*, 79−88.
42. Chen, X., Cook, R. K., and Rubenstein, P. A. (1993) *J. Cell Biol. 123*, 1185−1195.
43. Erickson, H. P., Taylor, D. W., Taylor, K. A., and Bramhill, D. (1996) *Proc. Natl. Acad. Sci. U.S.A. 93*, 519−523.
44. Lowe, J., and Amos, L. A. (1998) *Nature 391*, 203−206.
45. Yifrach, O., and Horovitz, A. (1995) *Biochemistry 34*, 5303−5308.
46. Roobol, A., Grantham, J., Whitaker, H. C., and Carden, M. J. (1999) *J. Biol. Chem. 274*, 19220−19227.
47. Admiraal, S. J., and Herschlag, D. (1995) *Chem. Biol. 2*, 729−739.
48. Maegley, K. A., Admiraal, S. J., and Herschlag, D. (1996) *Proc. Natl. Acad. Sci. U.S.A. 93*, 8160−8166.
49. Srikakulam, R., and Winkelmann, D. A. (1999) *J. Biol. Chem. 274*, 27265−27373.
50. Thulasiraman, V., Yang, C. F., and Frydman, J. (1999) *EMBO J. 18*, 85−95.
51. Horwich, A., Low, K., Fenton, W., Hirshfield, I., and Furtak, K. (1993) *Cell 74*, 909−917.
52. Lorimer, G. (1996) *FASEB J. 10*, 5−9.
53. Ewalt, K. L., Hendrick, J. P., Houry, W. A., and Hartl, F. U. (1997) *Cell 90*, 491−500.
54. Monod, J., Wyman, J., and Changeux, J. P. (1965) *J. Mol. Biol. 12*, 88−118.
55. Hlodan, R., Tempst, P., and Hartl, F. U. (1995) *Nat. Struct. Biol. 2*, 587−595.
56. Mattingly, J. R. J., Torella, C., Iriarte, A., and Martinez-Carrion, M. (1998) *J. Biol. Chem. 273*, 23191−23202.
57. Coyle, J. E., Texter, F. L., Ashcroft, A. E., Masselos, D., Robinson, C. V., and Radford, S. E. (1999) *Nat. Struct. Biol. 6*, 683−690.
58. Shtilerman, M., Lorimer, G. H., and Englander, S. W. (1999) *Science 284*, 822−825.
59. Cliff, M. J., Kad, N. M., Nicky, H., Lund, P. A., Webb, M. R., Burston, S. G., and Clarke, A. R. (1999) *J. Mol. Biol. 293*, 667−684.
60. Llorca, O., McCormack, E. A., Hynes, G., Grantham, J., Cordell, J., Carrascosa, J. L., Willison, K. R., Fernandez, J. J., and Valpuesta, J. M. (1999) *Nature 402*, 693−696.

BI992110S